A l'heure actuelle, les incertitudes sur la position du satellite ne permettent pas de réduire cette porte au-dessous de 10μs ; exceptionnellement, et dans les cas difficiles on pourra essayer 5μs.

Le tableau suivant fournit les probalités de "faux échos" dans les conditions précédentes

Bruits internes $10^3 \times 10^{-5}$	10^{-2}
Ciel nocturne sans lune $1{,}7\ 10^2 . 10^{-5}$	$1.7\ 10^{-3}$
Ciel nocturne à 20° de la pleine lune $5.10^2.10^{-5}$	$5\ 10^{-3}$
Ciel nocturne à 10° de la pleine lune $2.5\ 10^3. 10^{-5}$	$2.5\ 10^{-2}$
Satellite D_1 éclairé $1{,}7\ 10^2. 10^{-5}$	$1.7\ 10^{-3}$
Lune éclairée dans le champ $5.10^7. 10^{-5}$	$5\ 10^{-2}$
Ciel diurne $1.7\ 10^8 \times 10^{-5}$	$1.7\ 10^{-3}$
Fluorescence du laser 5nS après l'émission $10^4. 0$	0
Etoile polaire dans le champ $610^3. 10^{-5}$	$6\ 10^{-2}$

Ces différents bruits étant indépendants, il faut additionner les probabilités de "faux échos" dans chaque condition de tir. Cette porte est donc en principe suffisante dans de bonnes conditions de tir (nuit assez loin de la lune), et avec des éphémérides précises. C'est effectivement le procédé employé par beaucoup de stations.

I.2.2.2.b Détection de niveau

Ce procédé classique revient à réduire le gain de l'ensemble de la collection et de la détection.

On diminue l'amplitude de l'ensemble du signal bruité et l'on fixe un seuil qui sélectionne statistiquement le signal seul.

La courbe ci-dessous représente la probalité de répartition des photoélectrons de bruit en fonction de leur niveau.

Si U représente cette moyenne, on voit par exemple que la probabilités pour avoir des impulsions de bruit de niveau V = 2 U est de 10^{-2}

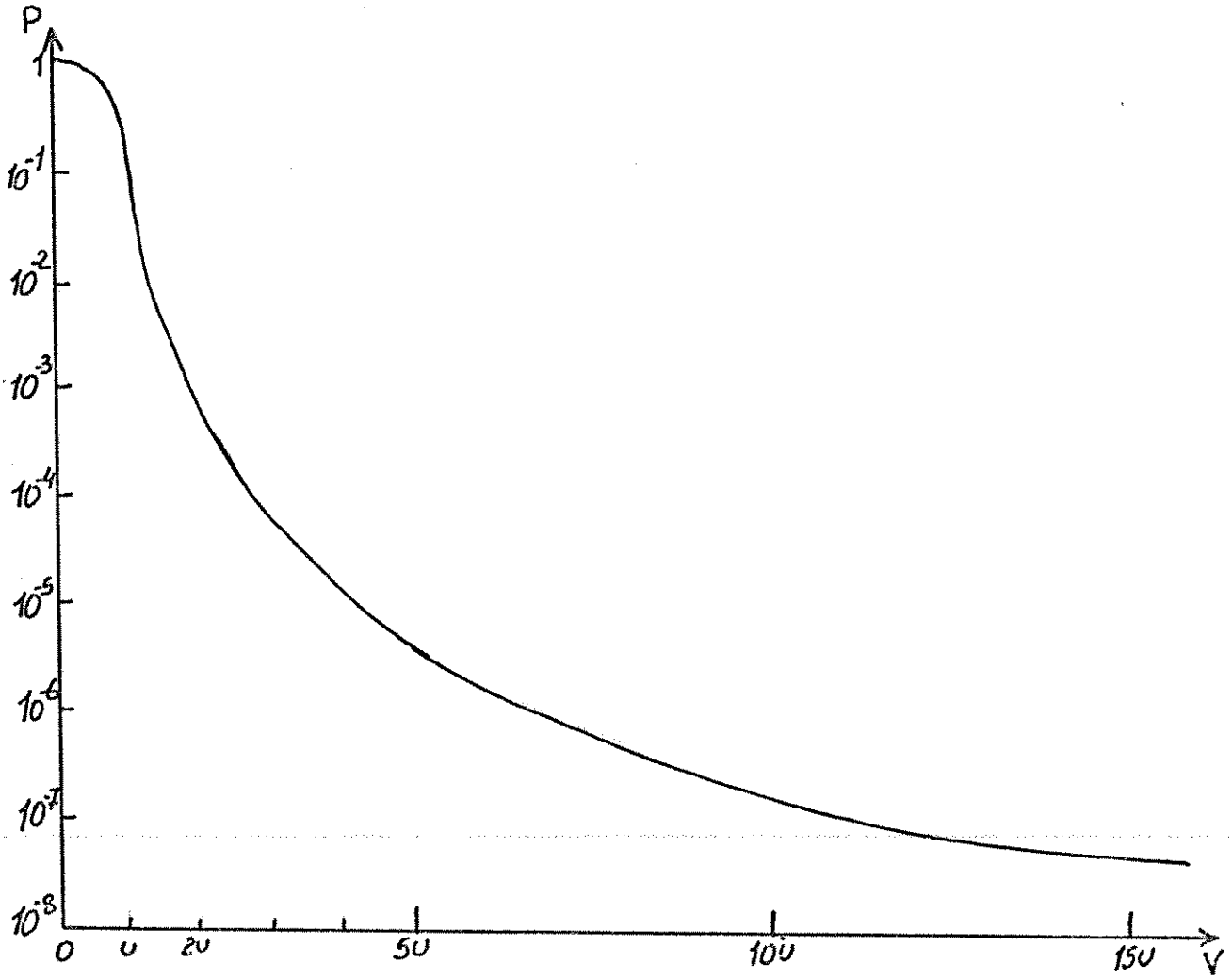

P probalité pour qu'une impulsion de niveau donne V apparaisse

U niveau moyen des impulsions de bruit

Si nous appelons : p la probalité désirée de faux écho

t le temps d'ouverture de la porte

P la probalité pour qu'une impulsion de bruit dépasse le niveau V

M la fréquence moyenne d'apparition des impulsions de bruit

Nous avons la relation

$$MtP = p \quad \text{ou} \quad P = \frac{p}{Mt}$$

Si par exemple nous prenons

$p = 10^{-2}$ $t = 100\,\mu s$ $M = 10^{4}$ photoélectrons s^{-1}

$$P = \frac{10^{-2}}{10^{4} \times 10^{-4}} = 10^{-2}$$

Sur la courbe nous obtenons V = 2 U

Pour avoir V = 2 U il faut qu'il y ait au moins deux photoélectrons superposés pendant le temps de retour de l'impulsion laser.

Cette impulsion est au moins égale à la largeur de l'impulsion laser émise qui est elle-même beaucoup plus large, en général, que les impulsions de bruit du photodétecteur.

Ceci signifie que dans le meilleur des cas (impulsion émise très courte ($\leqslant$ 1nS) et fonction de transfert du satellite très étroite) il faut deux fois plus de photons de retour que dans une détection simple. En général, pour des impulsions laser plus longues et (ou) une mauvaise fonction de transfert du satellite le facteur multiplicatif est beaucoup plus important (un traitement mathématique voisin de celui développé pour les coïncidences peut être fait. Il faut noter que si le signal reçu est très puissant, c'est à dire si les photoélectrons ne sont pas séparés, le rapport est effectivement égal à 2. Comme nous allons le voir, à réduction de portée égale ou inférieure, le bruit admissible par une coïncidence à 2 photoélectrons est beaucoup plus important que celui admis par une détection de niveau de rapport 2.

I.2.2.2.C Auto déclenchement d'une porte par l'impulsion de retour

Nous grouperons dans cette rubrique plusieurs procédés :

- système de coïncidence temporelle
- système de coïncidence spatiale
- système de coïncidence mixte spatio-temporelle

Ces méthodes mettent à profit la très grande concentration temporelle de l'émission d'un laser déclenché.

I.2.2.2.C.a. Coïncidence temporelle

Le principe est de n'accepter un signal que s'il présente la caractéristique de comporter au moins n photoélectrons pendant une durée égale ou très légèrement supérieure à celle de l'impulsion de retour.

Le signal issu du photodétecteur est divisé en deux. Une des voie attaque un circuit de mise en forme qui fournit une impulsion de sortie normalisée à une largeur légèrement supérieure à la durée de l'impulsion de retour prévue.

La seconde voie après passage dans une ligne à retard attaque une porte commandée par le signal mis en forme.

L'impulsion de la seconde voie doit se présenter à l'entrée de la porte juste avant celle venant de la première voie, de sorte qu'il n'y ait d'impulsion en sortie que si l'impulsion du photodétecteur est, soit : plus large que celle de bruit, soit multiple dans le temps d'ouverture

Schémas

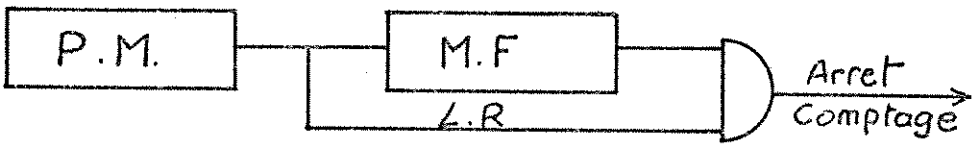

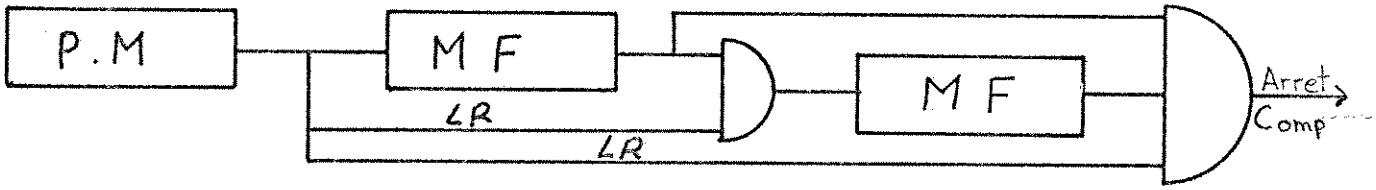

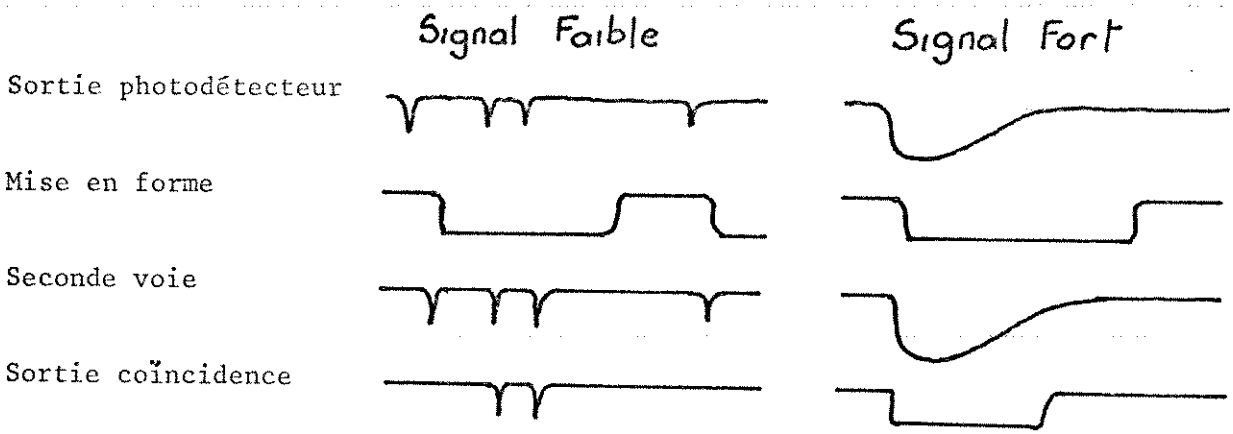

Si nous admettons que l'émission du photodétecteur est un processus de Poisson.

Le nombre q d'électrons émis dans l'intervalle Θ a pour moyenne $M\Theta = p$ (M bruit moyen du photodétecteur en impulsions s^{-1}) et pour probalité d'apparition $\pi(q) = e^{-p} \frac{p^q}{q!}$

La probalité de fausse alarme dans un intervalle est donc

$$P_\Theta(q \geq n) = \sum_{q=n}^{q=\infty} \pi = \sum_{q=n}^{q=\infty} e^{-p} \frac{p^q}{q!}$$

Si on admet que dans le temps d'ouverture t il y a $\frac{t}{\Theta}$ intervalles élémentaires indépendants, la probalité globale de faux écho est :

$$P_\Theta = \frac{t}{\Theta} e^{-p} \frac{p^n}{n!} \quad \text{ou} \quad p = M\Theta$$

I.2.2.2.C.b Coïncidence spatiale

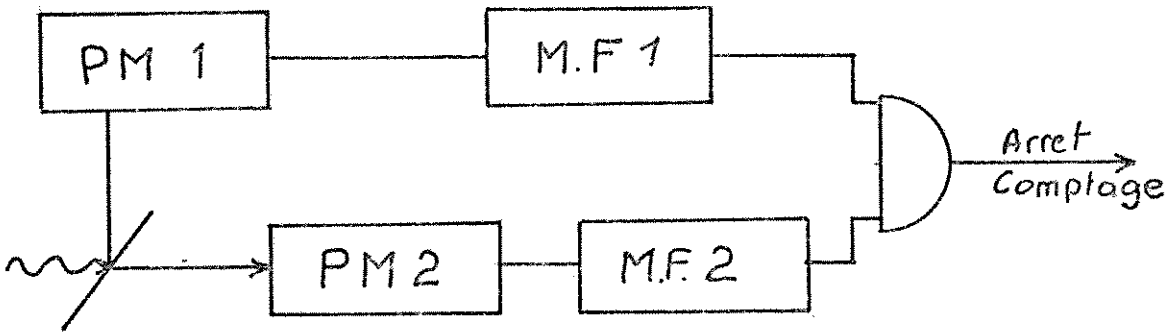

le faisceau de retour est distribué sur deux photodétecteurs. Les signaux issus de chacun d'eux sont mis en forme puis attaquent une coïncidence à 2 voies.

Il est possible par ce procédé d'effectuer des coïncidences sur plus de 2 photoélectrons en répartissant le faisceau sur plus de 2 photodétecteurs. On notera que chaque photodétecteur ne reçoit plus que la moitié du flux collecté, ce qui permet de doubler la fréquence de bruit sans saturer le photodétecteur tant du point de vue électronique (impulsions de bruit discrètes), que du point de vue électrique (dissipation maximum).

Si nous supposons, comme précédemment, que l'émission des électrons suive une loi de Poisson et que tout électron émis soit détecté. Si le signal reçu comporte P électrons et si le détecteur nécessite n électrons, le possibilité de manquer le signal :

$$P'_n = \sum_{K=0}^{K=n-1} e^{-p} \frac{p^K}{K!}$$

Si l'on divise ce signal en deux pour attaquer deux détecteurs fixés à n/2 électrons (n pair), et dont on exige que les deux se déclenchent, la probabilité de manquer le signal devient :

$$P''n = 1 - \left(1 - e^{-p/2} \sum\right)^2 \quad \text{avec} \quad \sum = \sum_{p=0}^{n/2-1} \frac{\left(\frac{p}{2}\right)^K}{K!}$$

$$P''n = 2e^{-p/2} \sum - e^{-p} \sum^2$$

Soit, dans le cas où n=2

$$P'_2 = e^{-p}(1+p) \qquad P''_2 = 2e^{-p/2} - e^{-p}$$

$$\frac{P''_2}{P'_2} = \frac{2e^{p/2-1}}{1+p}$$ toujours supérieur à 1

En particulier, en limite de portée où P est égal à 2

$$P'_2 = 3\ e^{-2} \simeq 0,4$$

$$P''_2 = 2\ e^{-1} \simeq 0,6$$

Nous n'effectuerons pas le calcul pour un système où la division est supérieure à 2 (équivalent de la détection sur coïncidences temporelles n > 2) car le montage devient assez complexe et le rapport de sensibilité décroît encore.

Par contre, un système à coïncidence spatiale présente aux bruits une protection plus efficace car les émissions de deux photomultiplicateurs ne sont pas absolument pas corrélées. En effet, l'émission électronique d'une photocathode n'obéit pas parfaitement à une loi de Poisson, il y a au contraire une émission de "rafales d'électrons".

I.2.2.2.C.c Coïncidence spatio temporelle

Dans le schéma de la coïncidence spatiale précédent on impose à chaque photodétecteur de fournir au moins une impulsion de signal durant l'intervalle $\ominus$.

Si An représente le $n^{ème}$ signal issu du 1er photodétecteur pendant un intervalle $\ominus$.

Si Bn représente le $n^{ème}$ signal issu du $2^{ème}$ photodétecteur, le signal d'arrêt du chronomètre C peut être représenté dans l'intervalle $\ominus$ par :

$$C = (A_1 + A_2 \ldots\ldots + A_1 \ldots\ldots) \cdot (B_1 + B_2 + B_3 \ldots\ldots B_n \ldots)$$

En limite de portée, le minimum imposé est :

$C = A_1 \cdot B_1$ (coïncidence spatiale à 2 voies)

On peut revenir à la sensibilité de la coïncidence temporelle à 2 photoélectrons en représentant le signal d'arrêt C par

$$C = A_1 \cdot B_1 + A_1 \cdot A_2 + B_1 B_2$$

C'est à dire que l'arrêt ait lieu

Soit si la coïncidence spatiale fonctionne

$$C = A_1 \cdot B_1$$

Soit si une coïncidence temporelle sur un des 2 photodétecteurs fonctionne

$$C = A_1 \cdot A_2$$

$$C = B_1 \cdot B_2$$

Le schéma suivant est un exemple possible de réalisation de ce circuit

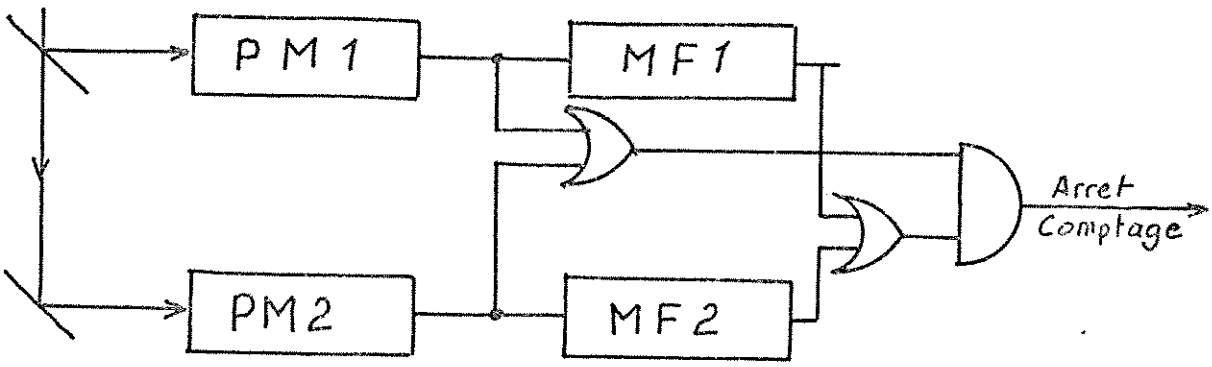

Cette méthode combine en grande partie les avantages des deux procédés et peut être généralisée à plus de 2 photoélectrons.

L'optique de reprise est mécaniquement prévue pour réaliser un système à deux voies et permet donc l'adaptation de coïncidences

soit, temporelle sur 2 ou 3 photoélectrons
soit, spatiale sur 2 photoélectrons
soit, spatio temporelle sur 2 à 6 photoélectrons

II. DETERMINATION DE LA PRECISION

On peut séparer les erreurs en deux groupes :

II.1. Erreurs Systématiques

II.2. Erreurs Aléatoires

II.1. Erreurs Systématiques

II.1.1. Erreur sur la vitesse de la lumière

Les résultats obtenus sont en secondes-lumière, la conversion en unités métriques s'obtient avec une erreur de l'ordre de 10^{-8} actuellement.

II.1.2. Fréquence de l'oscillateur local

Cet oscillateur pilote tant la chronométrie que la garde temps de la station horaire. Sa stabilité est de l'ordre de 10^{-13} (Cesium). L'erreur de chronométrie qui en résulte sur satellite est extrêmement faible $\ll$ à 1mm.

II.1.3. Définition de la grandeur mesurée

Ni la station, ni le satellite ne sont ponctuels, pour le satellite on portera une correction moyenne, en tenant compte de la position des réflecteurs par rapport au centre de gravité.

Des satellites tels que STARLETTE ou LAGEOS ont été étudiés pour minimiser cet effet et l'incertitude est réduite à des valeurs aussi faibles que quelques mm. Ce sont ces satellites qui doivent permettre l'évaluation de la précision de la station.

D'autre part, le point de référence fixe de la station est choisi à la croisée des deux axes. Ce point a un mouvement par rapport à l'embase de la tourelle très inférieur au mm.

II.1.4. Synchronisation horaire

Il est évident que la datation de l'heure de tir est extrêmement importante.

La solution actuelle est de se synchroniser sur un étalon connu.

Les moyens actuels permettent de synchroniser l'heure station sur le Temps Atomique à une valeur inférieure à 1 μs dans les pays développés (Europe, Amérique du Nord) par les méthodes de synchronisation télévision ou par le réseau Loran C.

La vitesse radiale des satellites étant au maximum de 5km s^{-1} ceci introduit une erreur externe à la station de télémétrie, égale à 0.5 cm. Dans les pays ayant un support technique horaire moins développé, un oscillateur "Cesium" associé à une synchronisation VLF et à des transports d' heure relativement fréquents (1/mois) doit permettre de déterminer l'heure des tirs par rapports au TUC avec un écart inférieur à 2 μ s (soit un ΔD $<$ 1 cm).

II.1.5. Réfraction troposphérique

Il serait illusoire de concevoir des stations de télémétrie laser ayant une précision de quelques décimètres, à fortiori de quelques centimètres,

si les perturbations inconnues introduites par la réfraction troposphérique étaient plus importantes.

Un certain nombre d'études ont été entreprises à ce sujet, en particulier par H.S. Hopfield. Les résultats suivants sont tirés de ses hypothèses et résultats.

Le passage de l'impulsion optique à travers la troposphère, introduit un accroissement de la durée du trajet. La connaissance de l'indice de réfraction le long du chemin optique fournit la correction à apporter sur la distance mesurée. L'étude de H.S.Hopfield permet de déterminer cette correction en fonction des conditions météorologiques locales.

Soit N l'indice de réfraction de la troposphère en un point. Nous le diviserons en deux composantes Nd et Nw, composante sèche et humide de cet indice local.

$$N = Nd + Nw$$

$$\text{ou} \quad Nd = \frac{77,6}{T} P$$

$$Nw = 3,73.10^5 \frac{e}{T^2}$$

avec P : pression totale en millibars.

e : pression partielle de la vapeur d'eau en millibars.

T : température absolue en °K.

Si nous admettons une décroissance linéaire de la température en fonction de l'altitude, la fraction sèche de l'indice de réfraction s'exprimera par la formule :

$$Nd = N_o d \left[\frac{\frac{T_o}{\alpha} - H}{\frac{T_o}{\alpha}} \right]^{\mu}$$

où $\mu = \frac{9}{R\alpha} - 1$

$N_o d$ et T_o : indice de réfraction et température de la surface au niveau O (niveau de la mer).

α : le coefficient de crécroissance de la température

R : constante de gaz : PV = RT

avec α = 6,8°C/Km et μ = 4

$$Nd = \frac{N_s d}{(hd-hs)} (hd-h)^4 \qquad h \leqslant hd$$

de la même façon

$$Nw = \frac{N_s w}{(h_N-hs)} (hw-h)^4 \qquad h \leqslant hw$$

où les indices s correspondent aux conditions au sol qui peuvent être différentes de celles du niveau de la mer. hd et hw les altitudes équivalentes pour lesquelles Nd et Nw deviennent respectivement nuls.

On déduit de ces formules les temps de trajet :

$$\int_{hs}^{hd} Nd \; dh = \int_{hs}^{hd} \frac{N_s d \; (hd-hs)}{5}$$

$$\int_{hs}^{hd} Nw \; dh = \int_{hs}^{hd} \frac{N_s w \; (hw-hs)}{5}$$

Les facteurs hd et hw de ces équations théoriques sont ajustées en utilisant la méthode des moindres carrés de façon à rendre compte des résultats expérimentaux avec la meilleure approximation possible.

Les valeurs trouvées sont de la forme :

$hd = h_o + a_d$ TC où $h_o d$ est la valeur de hd quand la température au sol est de 0°C

ad est le coefficient de température de hd TC en °C

Les valeurs numériques sont les suivantes :

hd = 40,082 Km

ad = 0,14898 Km/°C

de même

$hw = h_o w + a_w$ TC

avec

$h_o w = 13{,}268$ km

$a_w = -0{,}09796$ km/°C

Ceci fournit la valeur zénithale du temps de trajet à travers la troposphère avec une précision de quelques mm sur la composante sèche $\int Nd\ dh$ de quelques cm sur la composante humide $\int N_w dh$ l'ensemble $\int N\ dh$ étant déterminé à 1% sur une valeur zénithale de l'ordre de 2,5 m.

Depuis cette étude d'autres ont été réalisées, tenant compte non seulement des conditions locales au niveau de la station, mais aussi des conditions au sol autour de cette dernière (10 à 50 km), ce qui permet d'établir un modèle d'atmosphère anisotopique. La correction de réfraction peut alors être calculée avec une précision de quelques millimètres.

II.1.5. Constante d'étalonnage

Un certain nombre de retards électroniques existent dans la station et se compensent plus ou moins. La somme de ces retards fournit la constante d'étalonnage ou décalage fixe de la grandeur mesurée.

L'étude de la précision d'appareillage de la station se fait en négligeant tous ces facteurs qui déforment l'orbite d'un satellite de plusieurs façons :

- soit, par une homotélie par rapport à la station dans le cas d'erreur sur la vitesse de la lumière ou d'écart de fréquence de l'oscillateur local.

- soit, par un biais constant lors d'erreur de définition de la grandeur mesurée et de la constante d'étalonnage.

- soit, par un décalage des noeuds ascendants de l'orbite dans le cas d'erreur de datation

II.2. Erreurs Aléatoires

La mesure est le temps entre le centre de l'impulsion de départ et celui de l'impulsion de retour.

Si nous prenons $e^{-P} = 1$ ($M\Theta \ll 1$) et limitons le développement au premier terme

$$P(q \geq n) = \frac{P^q}{q!} \qquad donc$$

$$P_t = \frac{t}{\Theta} \frac{P^n}{n!} = \frac{t}{\Theta} \frac{(M\Theta)^n}{n!}$$

Calculons la limite de bruit admissible dans les mêmes conditions que la détection de niveau étudiée au paragraphe I.2.2.2.$_b$ soit :

$t = 100\mu s$ $P = 10^{-2}$ $n = 2$ et pour deux intervalles élémentaires $\Theta = 4nS$ et $\Theta = 12nS$ (Θ est la durée de la porte autodéclenchée)

$$M = \sqrt[n]{\frac{n!\,P}{\Theta^{n-1}\,t}}$$

$t = 100\mu s$ $P = 10^{-2}$ $n = 2$ $= nS$ $\longrightarrow$ $M = 2.2\ 10^5$

$t = 100\mu S$ $P = 10^{-2}$ $n = 2$ $= 12nS$ $\longrightarrow$ $M = 1.3\ 10^5$

(l'hypothèse $M\Theta \ll 1$) est bien vérifiée)

Les bruits admissibles sont donc beaucoup plus élevés que pour une détection de niveau qui, dans pratiquement tous les cas, amène une perte de portée de loin supérieure.

Si nous adoptons les valeurs limites pratiques suivantes :

$t = 100\mu s$ $P = 10^{-2}$ $n = 3$ $= 3nS$

On en déduit M maximal égal à 4.10^6

$t = 10\mu S$ $P = 10^{-2}$ $n = 3$ $= 3nS$

M devient voisin de 10^7

donc, sauf en tir de jour ou avec la lune éclairée dans le champ la probabilité de faux écho est très faible.

En réalité, le raisonnement ci-dessus néglige le fait que les intervalles Θ divisant t sont juxtaposés alors que l'instant initial d'un intervalle Θ susceptible de comprendre plus de n photoélectrons est en fait quelconque. Le calcul exact donne :

$$P_t = \frac{t}{\Theta} \frac{p^n}{(n-1)!}$$

Ce calcul simplifié fournit donc un calcul optimiste d'un facteur égal au nombre de photoélectrons choisi dans la coïncidence.

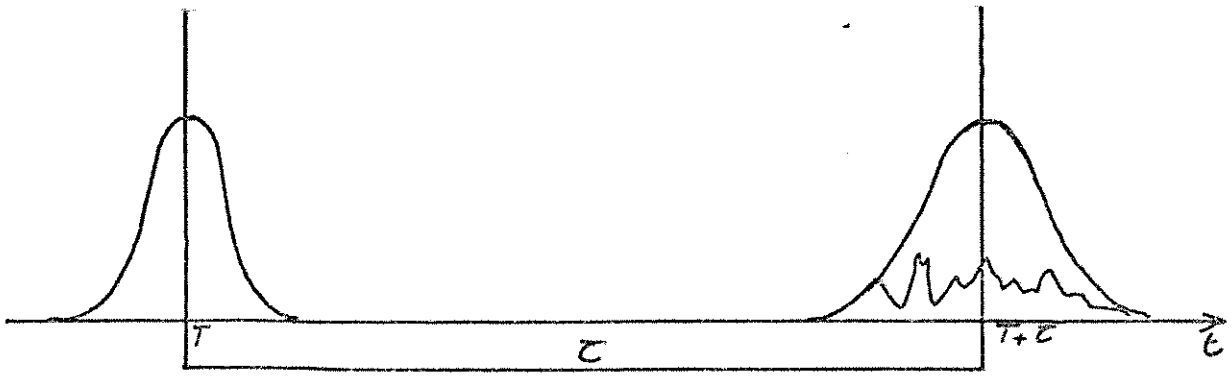

Si nous supposons qu'aucun phénomène aléatoire n'intervient, la forme de l'écho est celle de départ convaluée par la fonction de transfert du satellite cible. Si nous admettons que les deux sont des phénomènes Gaussiens, le temps de mesure est le temps pris entre les deux centres des courbes. Ces deux datations sont tributaires de variations aléatoires.

II.2.1. Déclenchement de la chronométrie

Nous avons adopté un système de détection centroïde. Pour cela, nous intégrons l'impulsion qui est ensuite distribuée sur 2 voies de rapport de tension 1 à 2. La voie de niveau le plus haut est retardée d'une durée au moins égale à celle de l'impulsion. Un comparateur rapide génère une impulsion au croisement des deux signaux

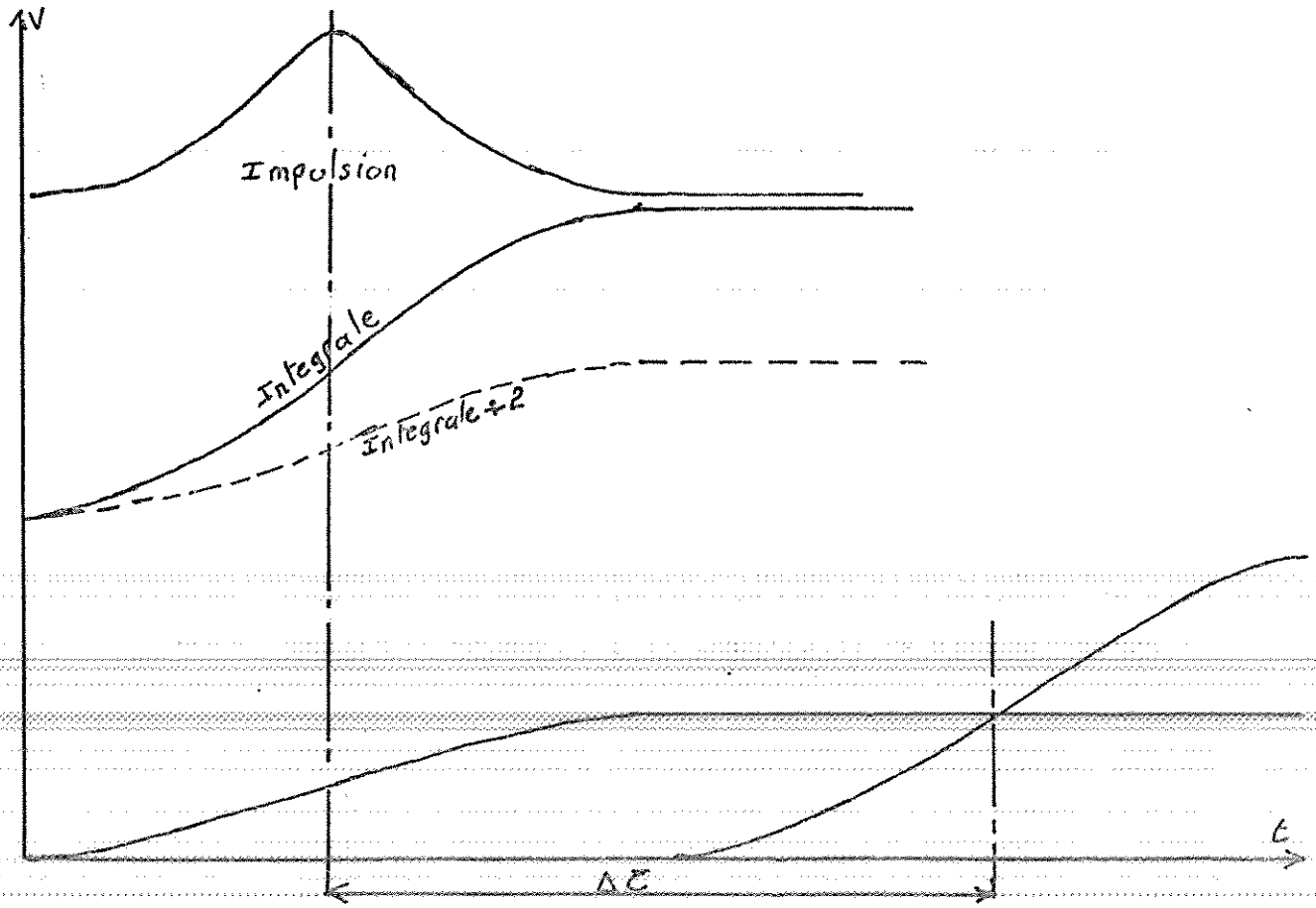

quel que soit le niveau de l'impulsion le moment daté est le centre de gravité de l'impulsion.

Les premiers essais du système réalisé à l'heure actuelle définissent un écart type sur $\Delta\tau$ de l'ordre de 50 PS pour des énergies laser variant de 2 à 15 j et des largeurs d'impulsion θ variant de 2 à 10 nS

II.2.2. Arrêt de la chronométrie

L'amplitude et la forme de l'impulsion de retour sont aléatoires. En cas d'échos faibles, cette forme peut même être représentée par des impulsions de photoélectrons uniques disjointes.

Dans le cas de fonctionnement sur des coïncidences, le déclenchement se produit sur le second photoélectron.

On peut estimer qu'en cas d'écho fait, on a un déclenchement avant le sommet avec un décalage moyen de $\frac{\theta}{3}$ et un écart type égal à $\frac{\theta}{10}$ en cas d'écho faible, le déclenchement se produit après le sommet avec un décalage moyen de + $\frac{\theta}{3}$ et un écart type égal à $\frac{\theta}{3}$

II.2.3. Erreur due à la résolution du compteur

Dans notre cas, le compteur a une résolution de 100 PS. Ceci signifie que l'on compte un nombre entier d'incréments de 100 PS. Si τ est un multiple de 100 PS nombre compté peut être la partie entière de ou cette quantité plus une unité. La répartition de l'erreur x (en PS) a pour densité de probabilité P (x) = 1-x et pour variance $\frac{1}{6}$ (écart type 17PS).

Le tableau suivant fournit donc les erreurs aléatoires calculées, suivant les conditions de tir. Pour réaliser ce tableau nous avons ajouté les variances des erreurs aléatoires, ce qui n'est pas vigoureusement valable.

	θ = 2nS	θ = 6nS	θ = 10 nS
impulsions fortes	3 cm	9 cm	15 cm
impulsions faibles	9 cm	30 cm	45 cm

Il doit être possible de diviser ces chiffres par un facteur 2 à 10 avec une analyse de l'écho de retour. Le facteur de division sera d'autant plus important que la quantité d'information donc le nombre de photons sera plus important.

Retour sur l'étalonnage

La détermination de la constante d'étalonnage peut être réalisée de trois façons différentes :

- mesure des retards électroniques et optiques dont la somme fournit la constante d'étalonnage.
- tirs sur cibles à distances connues en affaiblissant le signal suffisamment au retour pour simuler un écho sur satellite. La différence entre la valeur vraie de la distance et sa mesure par la station fournit la constante d'étalonnage.
- Réinjection par un appareillage optique (équerre optique, fibre de verre) d'une partie de l'énergie émise dans le télescope de réception. Ceci doit permettre un étalonnage interne et éventuellement une calibration à chaque tir.

III. CONDITIONS DE TIR

Nous avons défini trois conditions de tir :

III.1. Tir de nuit sur satellite visible en poursuite manuelle

Du point de vue télémétrie, cette condition est extrêmement facile à remplir. On peut déjà fonctionner avec un fitre relativement étroit (1,5 A°) et une simple détection.

Un système à coïncidence temporelle sur deux photoélectrons permet de travailler avec une porte large (plusieurs nS) et une très faible probabilité de faux échos facilitant grandement la validation des résultats et le traitement ultérieur.

La poursuite sera réalisée grâce à un "manche à balai" commandant la tourelle et à une visée optique à l'aide d'une lunette couplée à une caméra de télévision (Noticon) qui permettra, en limite de visibilité, de poursuivre un satellite de faible magnitude comme STARLETTE (12 à 13 cm)

II.2. Tir de nuit sur éphémérides

Les bruits étant les mêmes que précédemment il en est de même des résultats.

III.3. Tir de jour en automatique

Cette condition de tir n'est pas encore mise au point.

Néanmoins, en fonction de ce que nous avons analysé lors de l'étude des bruits il est possible de la remplir en adoptant un ou plusieurs des moyens suivants :

- réduction de la bande parasite du filtre interférentiel (étude et réalisation CERGA en cours)
- mise en service d'une coïncidence spatio-temporelle sur 3, 4, 5 ou 6 photoélectrons.
- détection de niveau en sortie des deux photomultiplicateurs.

La préférence est, bien sûr, donnée aux moyens qui réduisent peu la portée c'est à dire dans l'ordre où nous les avons classés ci-dessus.

CONCLUSION

Cette étude, non exhaustive, du choix des éléments de la station de télémétrie laser 2ème Génération, permet de mettre en évidence la définition des sous ensembles pour satisfaire aux exigences exposées au début de l'étude.

Ce choix ne limite pas la station à sa configuration minimale de départ et permet, sans interrompre son exploitation :

1er) d'augmenter sa précision par une étude de la forme de l'écho de retour

2ème) d'étendre la couverture, par une extension de périodes de tir (tir de jour) et par une réduction des domaines interdits (lune, voisinage du soleil).

THE SHORT-PULSE LASER-RANGING SYSTEM INSTALLED IN WETTZELL

P. Wilson, K. Nottarp, H. Seeger
Institut für Angewandte Geodäsie (Abtlg.II, DGFI), Frankfurt and
Sonderforschungsbereich 78, Satellitengeodäsie, der TU München
Fed. Rep. of Germany

HARDWARE DESCRIPTION

1. INTRODUCTION

In December 1974 the Institut für Angewandte Geodäsie, Frankfurt a.M., acting together with, and on behalf of the Sonderforschungsbereich Satellite Geodesy of the Technical University Munich, (SFB 78) placed an order with GTE-Sylvania, Mountain View, California, for an advanced laser ranging system. The contract was financed jointly by the Bundesministerium des Innern (Ministry of the Interior) and the Deutsche Forschungsgemeinschaft (German Research Council) through the Sonderforschungsbereich 78 and the system has been installed in Wettzell in a new building provided by the Institut für Angewandte Geodäsie, the stationary components being maintained in a climatically controlled environment.
The system characteristics are summarised in Tables 1 - 5.

2. PRESENT SITUATION

Following the difficulties experienced during the installation (see later discussions during the other sessions) the system is now being used daily for ranging to near-earth satellites such as GEOS-2 etc. No recent ranging results have been completely analysed, but first results obtained in Wettzell from Starlette (2 passes observed in June 1977) indicate a 5 cm noise level. A later pass observed to GEOS-A gave indications of discrete ranging with three distinct ranging intervals. These and other results will be presented during the symposium.

3. THE PROBLEM-AREAS ENCOUNTERED

The following summarises the main design problems which came to light during the first year of experience with the new system. These topics will be discussed in more detail during the subsequent sessions:

a) problems have been experienced with the laser power supply e.g. due to inadequate precautions against over-heating of the transformers in going from 60 Hz to 50 Hz operation;

b) the adjustment stability of the laser had to be upgraded;

c) problems are still being encountered with the surface loading on the optical components in the Coudé path;

d) an unsatisfactory coupling design gave rise to encoder damage;

e) the cable wrap proved to be poorly finished.

Apart from these design defects, the most significant time losses were suffered from

f) damage to the heat-exchanger, which occurred during transport from San Francisco to Frankfurt;

g) the search for a fault in the receiver electronics which prevented the recording of data for about five months.

Although we have been disappointed in the quantity of data delivered to date, we are optimistic for the future and look forward to making a significant contribution to future tracking campaigns.

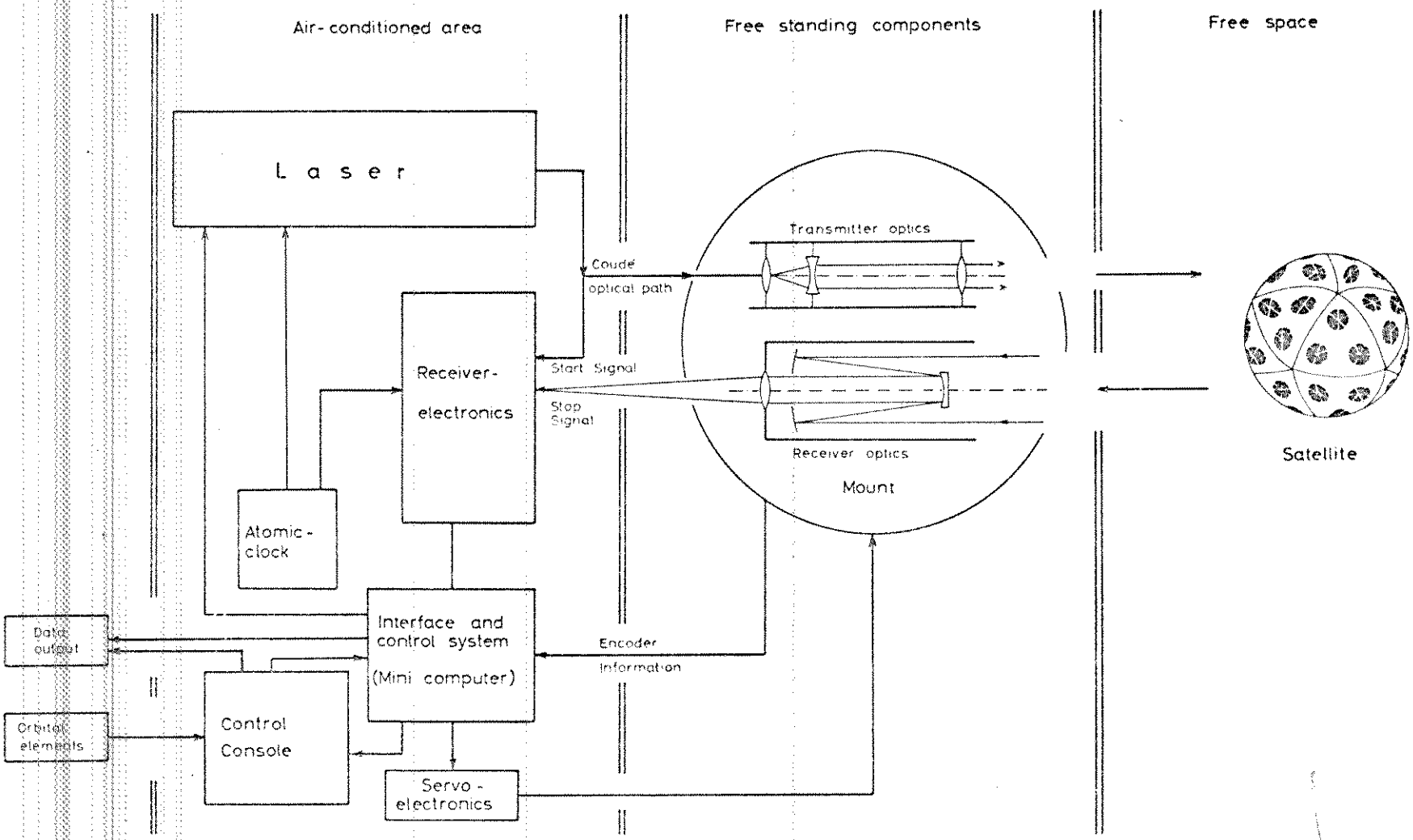

BLOCK DIAGRAM OF THE LASER-RANGER

Table 1. Summary of Specifications for Laser Ranging System

Original Specification	Original Proposal	Acceptance Tested
General		
Range 350 to 20 000 km	350 - 20 000 km	900 - 9000 km
Data recovery rate up to 1 range/sec	3 ranges/sec	up to 5 ranges/sec
Operating staff / 2 persons	2 persons	1 person
Mount		
Configuration alt-az. or x - y with Coudé axes	alt-az. with Coudé	alt-az. with Coudé
Angular travel - elevation 110° - azimuth 540°	190° 540°	190° 540°
Tracking		
Continuous from -10° through zenith to -10° under control of computer	Continuous from -10° to within 2° of zenith to -10° under computer control	Continuous from -10° to within 2° of zenith to -10° under computer control
Tracking rates from 1°/min to 1°/sec in plane of orbit	1°/min to 1°/sec	1°/min to 1°/sec
Orthogonality of rotational axes/±2"	±2"	1"
18 bit encoders	18 bit	18/20 bit
Transmitting Optics		
Effective beam divergence 0.1 to 5.0 mrad	0.1 to 5.0 mrad	0.025 to 2.0 mrad
Receiving Optics		
Cassegrain	Cassegrain	Cassegrain
Diameter 60 to 90 cm	61 cm	61 cm
FOV 1 to 15 arc	0.05 to 2.3 mrad	0.05 to 2.3 mrad
Laser		
Ruby or Nd-YAG	Ruby or Nd-YAG	Nd-YAG
Pulse transmission mode or mode-locked operation	PTM or mode-locked	mode-locked
Halfenergy pulse width/100 psec to 5 nsec	200 psec to 5 nsec	200 psec
Peakpower 1 to 2 GW	1 GW or 1.25 GW	1.25 GW
Natural divergence 1 mrad	1.2 to 6 mrad dependent on rep.rate, or 1 mrad	0.3 mrad
Spectral region - green or red, 694 nm or 532 nm	694 or 532 nm	532 nm
Pulse repetition rate/1pps or better	3 pps	4 pps
Receiver		
Electrostatic	Electrostatic	crossed-field
Rise time better than 2 nsec	≤ 2 nsec or 0.5 nsec	0.5 nsec
Pulse Analysis	if required	not required
Computer		
Data Storage on mag.-tape and/or disk	disk with 1.2 mio word capacity	disk
Imput-output-teletype, mag.-tape, punched tape	all three	mag.-tape, punched tape, printer
Memory - at least 16 K 16-bit words	16 K expandable to 127K	32 K

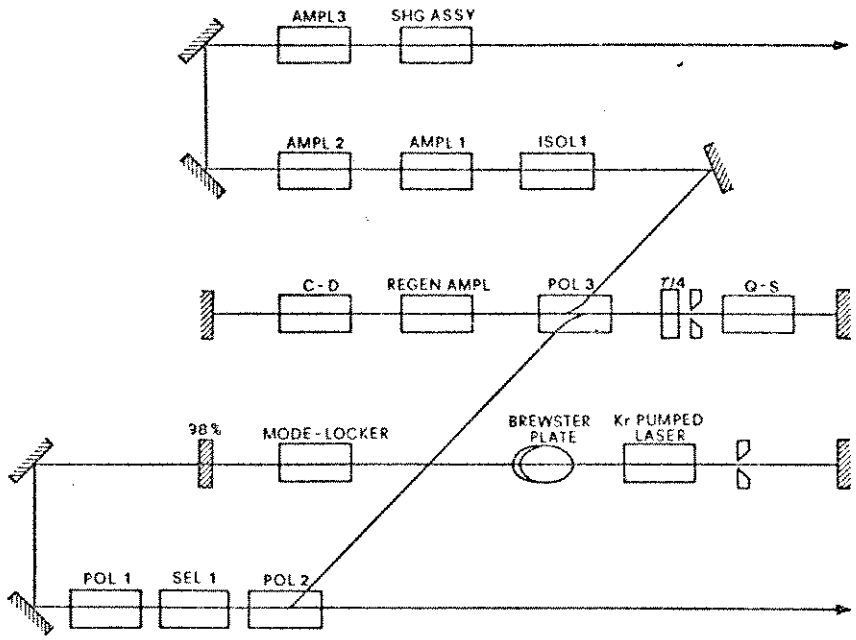

Figure 2. Block Diagram of the Optical Lay-Out of the GTE Sylvania Nd-YAG Laser

Table 2. Characteristics of the Frequency Doubled Nd-YAG Laser

Peak power output:	1.25×10^9 watts at 0.53 µm
Energy output:	0.25 joules per pulse at 0.53 µm
Output stability:	± 5 %
Pulsewidth:	Less than 0.2 nanoseconds
Repetition rate:	4 pulses per second
Beam divergende: (full angular-field containing 90 % of the energy)	Less than 10 times the diffraction limit from the final amplifier assembly
Beam diameter:	12 mm
Spectral linewidth:	Less than 2 nanometer
Spectral line stability:	Better than 0.1 nanometer
Spectral line position:	Repeatable to better than 0.1 nanometer from one operational cycle to another

Table 3. Specifications for the Positioning Mount

Rotational freedom in elevation	- 10° to + 190°
in azimuth	± 270°
Orthogonality of rotation axes	± 2 arc sec
Wobble on each axis	± 1 arc sec
Tracking velocity in elevation	0.5°/min to 2°/sec
in azimuth	0.5°/min to 32°/sec
Acceleration in elevation travel	$2°/sec^2$
in azimuth travel	$10°/sec^2$
Payload	500 kg
Static pointing accuracy	Better than 10 arc sec
Levelling and alignment in azimuth	Better than 1 arc sec
Prime power	220/380 V
Operating temperatures	- 20° C to + 50° C
Humidity	0 - 100 % without damage

Table 4. Specifications of the Optical Subsystems

Transmitting optics	
Configuration	Galilean
Magnification	12 x
Input diameter	16 mm
Output diameter	200 mm
Focus (divergence)	0.025 to 2.0 mrad
Alignment stability	10 °/o of divergence
Correction wavelengths	572, 643, 1064 nm
Peak power input	2 GW/cm^2
Optical coatings - maximum loss	0.25 °/o / surface
Receiver optics	
Configuration	Catadioptric Cassegrain
Aperture diameter	60 cm
Focal length	440 cm
Correction wavelength	532 nm
Alignment stability	10 arc sec over $\pm$ 20° C
Field of view	0.05 to 2.3 mrad
Sighting telescope	
Configuration	Maksutov - Cassegrain
Aperture	90 mm
Focal length	1 300 mm
Magnification	50 x
Field of view	55 arc min
Resolution	1.5 arc sec

Table 5. Specifications for the Varian 153A Static Crossed-Field Photomultiplier

Photocathode / window material	S-20/Sapphire
Cathode diameter	5 mm
Cathode quantum efficiency	10°/o typical at 530 nm
Gain	10^5 typical, 5 x 10^4 min.
number of stages	6
Dynode material	BeCu Alloy
Anode dark current	3 x 10^{-9} typical at 20°C
Output current	250 µA max. continuous
Bandwidth, 0 to -3 dB	DC to 2.5 GHz
Anode rise time (10 °/o to 90 °/o)	150 picoseconds

LUNAR RANGING MODIFICATIONS FOR THE LASER RANGING SYSTEM IN WETTZELL, FED. REP. OF GERMANY

Peter Wilson
Institut für Angewandte Geodäsie (Abtlg.II, DGFI), Frankfurt and
Sonderforschungsbereich 78, Satellitengeodäsie, der TU München
Fed. Rep. of Germany

HARDWARE

1. INTRODUCTION

Already prior to installation of the new laser ranging system in Wettzell it was recognized that the system has potentially the capability for ranging to the moon. The computation of the energy balance, assuming the laser to be operating at full energy, showed that the transmitted energy per second, divergence, receiver diameter and detector efficiency more than meet the minimum requirements for lunar ranging. However, to implement this capability a number of hardware modifications are necessary and the techniques for applying the system have to be defined.

2. HARDWARE MODIFICATIONS

The hardware modifications may be considered under the following grouping:

- changes in the computer interface unit, system control and modification of the servo amplifier to achieve the optimally smoothed low-rate pointing of the mount required for lunar ranging;
- introduction of a lunar range gate unit and modification of the system range timing counter to permit event timing, since some 12 laser pulses will be in flight before the return signal associated with the first one is detected;

- modification of the receiver control unit permitting operation in the normal satellite mode (using a range-time counter) and in lunar mode (event timing);
- introduction of remote mount control to permit fine pointing e.g. to stars, from the observers telescope position;
- reduction of the laser firing jitter from currently 125 msec to approx 150 μsec;
- upgrading of the photomultiplier by introduction of the newest Varian static crossed field unit, with 25 °/o guaranteed minimum quantum efficiency (35 °/o typical);
- introduction of a thermostatically controlled 10 Å narrow-band filter to replace the current 25 Å unit;
- introduction of a video tracker to permit optimal target pointing during the calibration procedures.

SOFTWARE

Besides the software support to be described implicitly during the session on calibration, an extensive software package is being developed in support of the lunar ranging modifications. This package is being planned as an independent operating system.

The lunar ranging procedures controlled by this software visualise the computation of the lunar ephemerides, system calibration, ranging execution, preliminary data processing and system diagnostics. The ranging execution consists of the selection of and pointing to a suitable star towards which the lunar reflector is moving, to determine the momentary differential offsets due to instantaneous refraction and optical deformations. The differential offset will then be extrapolated to the predicted lunar pointing angles to obtain the anticipated reflector position. In the event that returns are still not possible an automatic search pattern can be introduced.

LASER RANGING WORK AT THE GODDARD SPACE FLIGHT CENTER - AN UPDATE -

Thomas E. McGunigal
NASA/Goddard Space Flight Center
Code 723
Greenbelt, MD 20771

INTRODUCTION

A paper[1] which described the Goddard laser ranging systems was included in the Proceedings of the 2nd Workshop on Laser Ranging Instrumentation which was held in Prague in 1975. The purpose of this paper is to describe the current status of the laser ranging work at Goddard. There are two main thrusts to this work; 1) the development and operation of the network systems to meet operational requirements, and 2) advanced systems development and system improvement. Within the Goddard organization the network engineering and operations work is being done by the Networks Directorate and the advanced development is being done by the Engineering Directorate. The work being done in both directorates will be briefly summarized in this paper.

THE LASER TRACKING SUBNET

For the last several years the network activity has been in a period of dynamic growth. In 1975, one fixed and two mobile stations were in operation and by the end of 1978 the network will consist of one fixed and eight mobile stations. Although the systems are not identical, the fundamentals of system operation and the performance goals are the same as those described in the 1975 paper. The characteristics of the various systems are summarized in Table 1. The first three mobile systems were designed and integrated in-house at Goddard. The newest systems, Moblas 4-8, are two trailer systems consisting of the Mobile Optical Mount System (MOMS) developed for Goddard by Contraves Goerz Corporation, and the Electronics Van designed by Goddard's Networks Directorate. Systems integration and test are being done at Goddard with the Bendix Field Engineering Corporation as integration contractor.

Moblas 4-8 Characteristics

A. The Mobile Optical Mount System. The Mobile Optical Mount System has been described in detail by Economou et al[2]. Briefly, it consists of a trailer housing a two axis tracking mount including an 0.75 meter receiver telescope and a coude type transmit optical system with a 10cm clear aperature. The trailer also includes a transmitter compartment which is a class 10,000 clean room and additional space for laser power supplies and electronics racks. The mount compartment has a retractible roof and walls which deploy to form a working platform around the mount. The specified performance characteristics are summarized in Table II[2].

B. Laser Subsystem. The laser for the Moblas 4-8 systems is a frequency doubled Nd:YAG laser which was manufactured by General Photonics, Inc. It is a Q-switched laser with a 6 nanosecond pulsewidth and an output energy of 0.25 Joules at a wavelength of 532 nanometers. It has been designed to operate in any orientation and over a wide temperature range so that it can be mounted on the elevation axis of the telescope. A collimator is an integral part of the laser resulting in a beam divergence of 0.2 milliradians.

C.. Receiver Subsystem. The receiver subsystem is essentiallythe same as the earlier systems. It uses an Amperex 56TVP photomultiplier tube and a fixed threshold pulse discriminator in conjunction with a waveform digitizer for pulse position measurements. The waveform digitizer is a Tektronix 7912 system rather than the previously employed LeCroy WD-2000. The time interval unit is a Hewlett Packard 5360A computing counter.

D. Computer Subsystem. The Moblas 4-8 system's use a Mod Comp II computer unit with 16-bit word length and 64K BYTES of memory. The software package is being extensively revised to accomodate the new computer and to conform to Network standards for data format and satellite predictions. It is not complete at this writing so that no details are available.

E. System Status. The Moblas 4-8 systems are now in the process of final integration. System testing is presently scheduled for the Summer of 1978 with operational deployment planned to begin in the Fall.

ADVANCED SYSTEMS DEVELOPMENT

Advanced systems development at Goddard is being done by the Electro-Optics Branch in the Engineering Directorate. Facilities are available for both laboratory and field test work.

1. Field Facilities

The centerpiece of the advanced development activity is the 1.2 meter telescope located at the Goddard Optical Research Facility - four miles away from the central complex at Goddard. This telescope is illustrated in Figure 1.

The telescope employs a coude optical system with a 1.2 meter aperture, a focal ratio of f 26.3 and an equivalent focal length of 32 meters. The mirrors have polished aluminum surfaces on fused silica substrates. An indexable mirror within the pier at the couderoom level permits the light bundle to be quickly redirected through any one of eight ports to eight possible experiments. It is possible to reconfigure the telescope to a Cassegrain system to meet special requirements. Also,machined surfaces are provided on the elevation axis for mouting equipment directly to the telescope. Electrical connections to these areas are provided by a cable wrap and sliprings. The entire moveable structure rides on an azimuth axis air bearing. Precision roller bearings are used for the elevation axis. Each axis is equipped with a directly coupled torque motor, tachometer and 22-bit digital shaft angle encoder.

The system is controlled from an operator's console in the computer/control room or from an observer's position on the azimuth axis. A Honeywell 716 computer is interfaced to the telescope and to the operator's console and controls telescope pointing. This computer has a 16-bit word length and 48 thousand BYTES of memory. In addition to its realtime interfaces, it has two magnetic tapes, a line printer, card reader, typewriter and paper tape equipment. For satellite tracking the 716 computer generates telescope pointing commands in realtime from polynominals describing the satellites position.

Another function of the 716 is to model the structural and alignment errors of the telescope. Typical errors include a lock of orthogonality between the azimuth and elevation axes, sagas which vary with elevation angle, encoder offsets, coude mirror misalignments, etc. These errors are determined by observations of a well distributed series of 40 to 50 stars. A regression analysis is then performed to determine the coefficients of all the error terms in a mathematical model of the telescope. The model equations are evaluated during satellite tracking to correct the telescope pointing.

An Interdata 8/32 computer has been interfaced to the Honeywell 716. This machine has a word length of 32 bits and 384 thousand bytes of memory plus a 10 megabyte disc. A software system has been written which allows the two machines to exchange data and makes the line printer, card reader and magnetic tapes available to the 8/32. The 8/32 was added to provide more mathematical computing power. It will be used in realtime to correct the predicted satellite state vector on the basis of the actual range measurements in order to improve orbit prediction accuracy. In non-real time it will be used to analyze the ranging system measurement data.

In addition to software directly related to satellite ranging, the software system includes capabilities for solar, lunar, planetary and star tracking.

Two experiments which have an immediate bearing on the improvement of future laser ranging systems are currently in progress at this facility. The first of these is a more or less conventional ranging system using a 5 nanosecond pulsewidth cavity dump Nd:YAG laser producing 75 millijoules of energy at 532 nanometers. The receiver uses a static crossfield photomultiplier tube with a risetime of 200 picoseconds and a high performance constant fraction discriminator developed by Branko Leskovar and C.C. Lo at Lawrence Berkeley Laboratories[3]. The time interval unit is a Hewlett Packward 5370A with 20 picosecond resolution which was recently introduced. The purpose of this work is to test on a continuing basis under actual field conditions new ranging system components or concepts which might be of value to the network systems.

The second experiment is being conducted with NASA and Navy funding by Prof. Carroll Alley and others of the University of Maryland. The purpose of this work is to demonstrate the feasiblity of using single photoelectron ranging techniques for satellite ranging. He is using a 200 picosecond pulsewidth Nd:YAG laser which operates at 30pps and with less than a millijoule of energy per pulse at 532 nanometers.

2. Laboratory Facilities

Extensive laser laboratory facilities are available at Goddard but the precision ranging laboratory is uniquely equipped to perform state-of-the-art measurements of system or subsystem performances. This laboratory is shown schematically in Figure 2 . A wide range of laser sources, optical detectors, and ranging electronics are available. Single retroreflectors are mounted on water tanks and towers at nominal distances of 500 meters, 5KM meters and 22 KM permitting measurements through variable length atmospheric paths.

REFERENCES

1. T.E. McGunigal, W.J. Carrion, L.O. Caudill, C.R. Grant, T.S. Johnson, D.A. Premo, P.L. Spadin, G.C. Winston, Satellite Laser Ranging Work at The Goddard Space Flight Center. WESCON Technical Papers, Vol. 19, Section 9/2, pp. 1-8, 1975.

2. G.A. Economou, L.C. Mackey, S.A. Snyder, "Precision Long Range Laser Ranging System". To be published in the proceedings of the S.P.I.E. Conference Photo and Electro Optics in Range Instrumentation, March 12-15, 1978.

3. B. Leskovar, C.C. Lo, Optical Timing Receiver for the NASA Laser Ranging System, Part I: Constant Fraction Discriminator, Lawrence Berkeley Laboratory Report, LBL-4219, August 14, 1975.

TABLE I

PARAMETER	STALAS	MOBLAS I-III	MOBLAS IV-VIII
WAVELENGTH (Å)	5300	6943	5300
ENERGY/PULSE (J)	0.25	0.75	0.25
PULSE WIDTH (Ns)	0.2	5	5
RECEIVER APERTURE (M)	0.5	0.5	0.75
DIVERGENCE (Mr)	0.1	0.1	0.2
QUANTUM EFFICIENCY (%)	12	2.5	12
SYSTEM EFFICIENCY (%)	15	15	20

Table II
Summary of Mount Operational Parameters

Receive Optics:	30-inch clear aperture f/5 Cassegrain telescope f/1.5 primary mirror 15% optical loss 10% obscuration loss 80% of energy in 5 arc second blur over 5 milliradian field
Transmit Optics:	Five identical but independently adjustable mirrors allowing a 10 centimeter diameter transmission path from a stationary point off mount.
	Mirrors:
	λ/10 @ 532 nm 99.8% reflectivity at 532 nm 70% reflectivity between 450 and 650 nm 1.25 gigawatt energy and handling
Servo Performance:	20^{o}/sec. azimuth axis velocity 5^{o}/sec. elevation axis velocity 0.001^{o}/sec. minimum velocity, both axes $5^{o}/sec.^{2}$ azimuth axis acceleration $3^{o}/sec.^{2}$ elevation axis acceleration
Readout:	21-bit natural binary
Physical Measurements:	110 inches maximum height (telescope pointed to Zenith) 82 inches of height to elevation axis 9500 pounds of weight 45-inch azimuth swing radius 34-inch elevation swing radius 50 Hertz resonance (legs)
Pointing Accuracy:	Transmit optical system 12 arc seconds 3

48" APERTURE PRECISION TRACKING TELESCOPE

OF THE GODDARD OPTICAL RESEARCH FACILITY

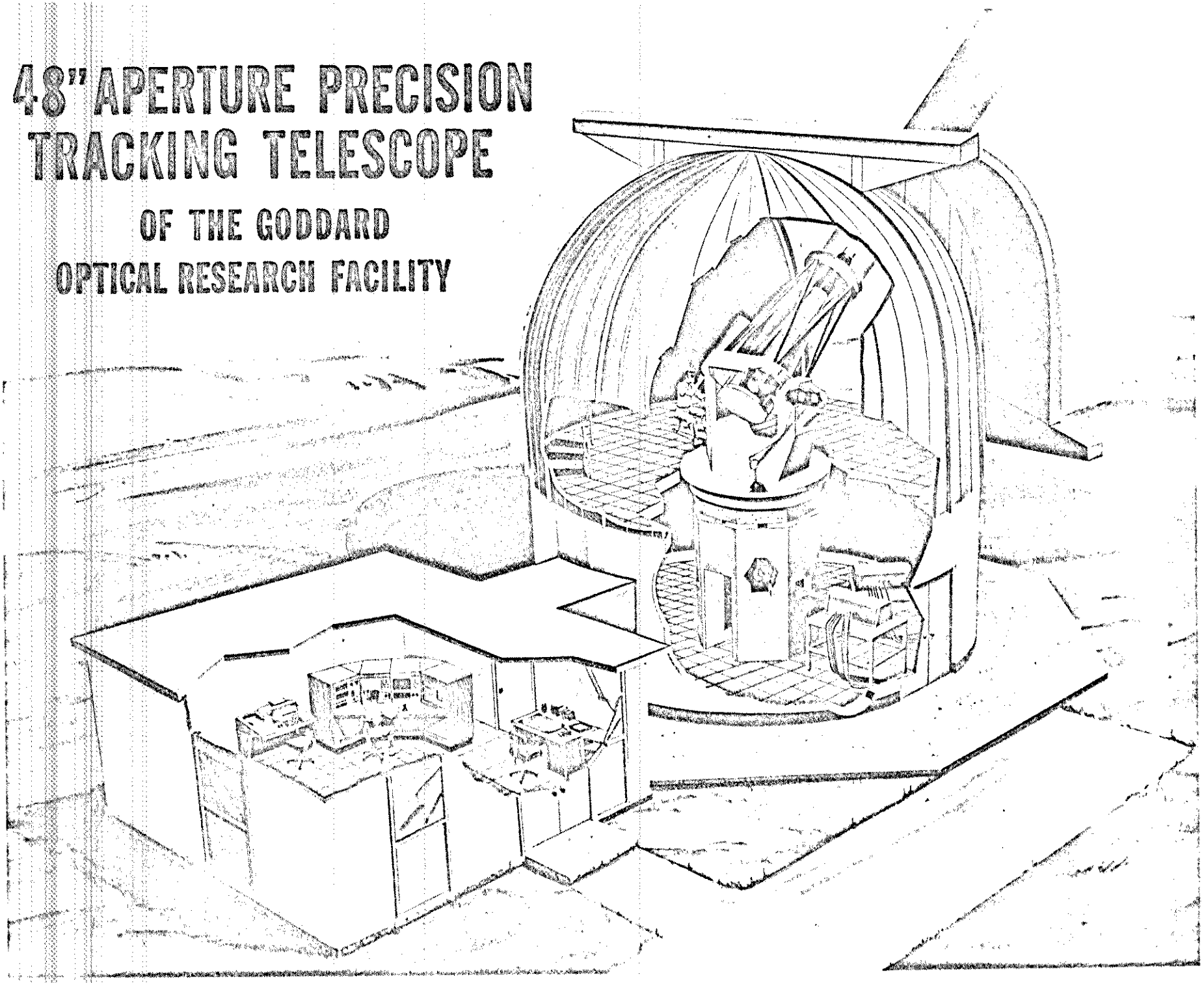

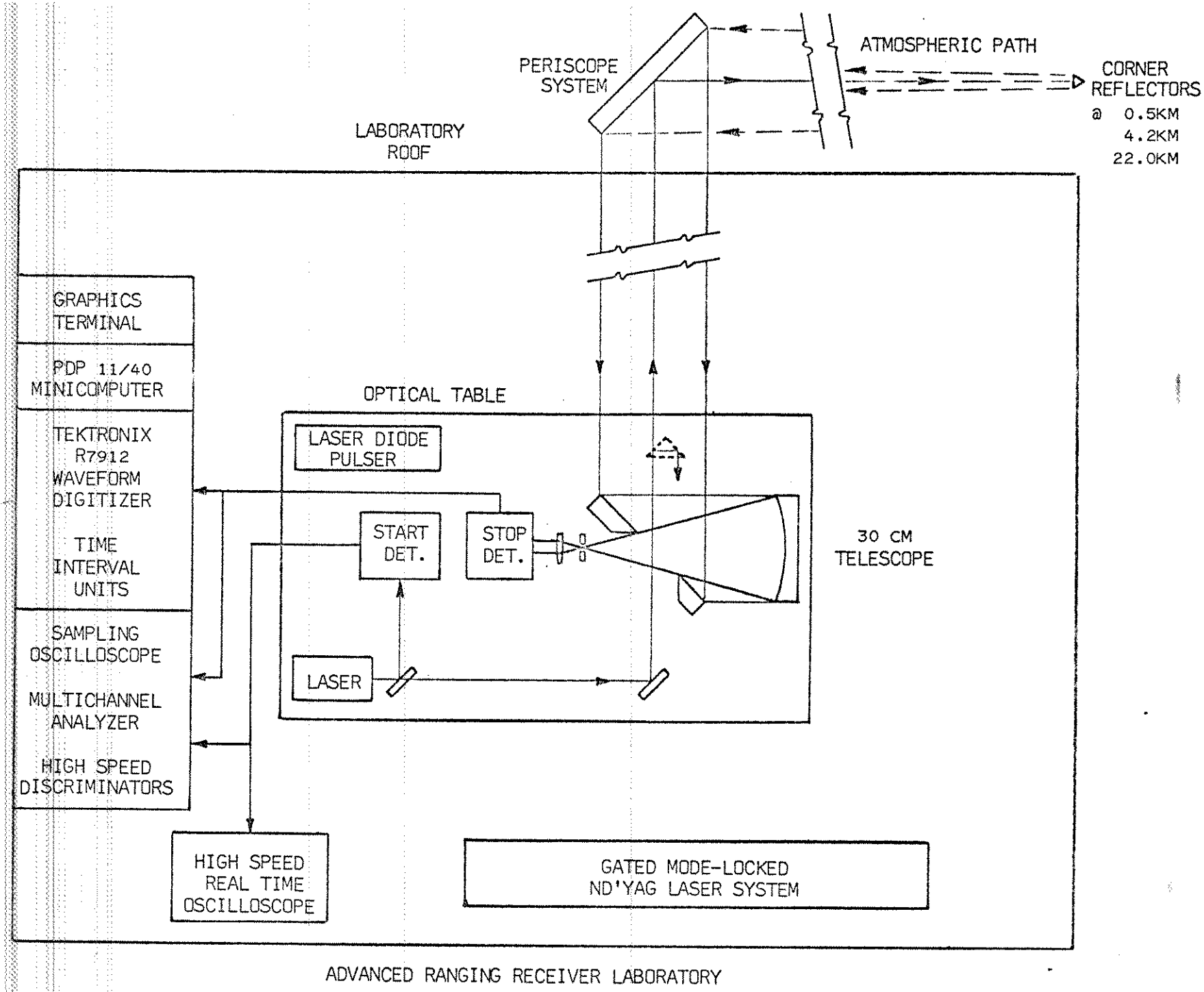
PERISCOPE SYSTEM
ATMOSPHERIC PATH
CORNER REFLECTORS
@ 0.5KM
4.2KM
22.0KM
LABORATORY ROOF
GRAPHICS TERMINAL
PDP 11/40 MINICOMPUTER
TEKTRONIX R7912 WAVEFORM DIGITIZER
TIME INTERVAL UNITS
SAMPLING OSCILLOSCOPE
MULTICHANNEL ANALYZER
HIGH SPEED DISCRIMINATORS
OPTICAL TABLE
LASER DIODE PULSER
START DET.
STOP DET.
30 CM TELESCOPE
LASER
HIGH SPEED REAL TIME OSCILLOSCOPE
GATED MODE-LOCKED ND'YAG LASER SYSTEM
ADVANCED RANGING RECEIVER LABORATORY

FIGURE 2

INTERKOSMOS LASER RADAR NETWORK

K.Hamal

Faculty of Nuclear Science and Physical Engineering
Brehova 7,Prague 1,Czechoslovakia

To fulfil the requirements of the Interkosmos program related to the projects of Long Arc Arctic Antarctic and the Long arc East West,the international Laser Radar Working Group and the Interkosmos Laser Radar Network has been built |1,2|.The accuracy $\pm$ 1.5 m and ranges up to 3000 km has been expected.

Twelve stations of the first generations have been build in the cooperation of CSSR,GDR,PRH,PRP,USSR,Cuba and have been operating together with ISRO in India,HIAG in Egypt,UMSA in Bolivia. One station is kept in Prague for training purposes.

The main performances are summarized in Fig.1.The expected retrosignal is shown.However,the measured signal was 10 times lower.The explanation is possible to find in the saturation efect of a PMT due to the scattering,especially when high humidity.The efect was examined and confirmed at Crimean observatory (station No.4) |3|.PMT was covered when the beam passes through the atmosphere.The description of the typical station is in |2|.The block scheme is on Fig.2.There are certain differences especially ref. to the mount,data output and time base.See Tab.1.Station No.2 is equiped by HP 30 desk top calculator |4|.The stations No.8 and 11 are equiped by SBG 2 mount.The station No.6 is equiped by a special mount.The upgraded station No.2 is described in |5|.The transportability aspect are desribed in |6|.The time interval measuring technique including the calibration is decribed in |7|.

Long arc fit using |8| SAO Differential Orbital Improvement Program with abbruated gravited field,residuals and the internal coherence are shown in Tab.2.

The photograph of the stationary station No.9 in Kavalure in India is on Fig.4.

The Interkosmos satellite laser network is shown on Fig.3.

References

|1| Masevitch A.G.,Abele M.,Almar J.,Daricek T.,Hamal K.,Kielek W., Navara P.,Novotný A.,Stöcher R.:Interkosmos Mobil Satellite Laser Ranging Observatory,Proceedings of the International Symposium on the Use of the artificial Satellites for Geodesy and Geodynamics,ed.G.Veis,Athens,1973,Publication of the National Technical University Athens,Greece,1974,p.81-96.

|2| Masevitch A.G.,Hamal K.:Interkosmos Laser Radar Stations,COSPAR,Philadelphia,1976.

|3| Štirberg L.C.,Preprint FJFI,No.77/30.

|4| Novotný A.:A Desk Top Calculator Control System for Laser Ranging,in the proceedings.

|5| Fahim at al.A Joint INTERKOSMOS/SAO/HIAG Laser Project,to be presented on 2.International Symposium The Use of Artificial Satellites for Geodesy and Geodynamics,Athens,June 1978.

|6| Hamal K.,Consideration for a Transportable System,in this proceedings.

|7| Kielek W.,Signal Processing,in this proceedings.

|8| Pearlman M.R.,private communication.

Figure Capture

Fig.1. (a) The calculated retrosignal based on radar equation.
(b) Characteristics of the Interkosmos stations.

Fig.2. Block scheme of the station No.10.

Fig.3. Interkosmos Laser Radar Network May 1978.

Fig.4. The photograph of the station No.9.

Tab.1. INTERKOSMOS LASER RADAR NETWORK MAY 1978

No.	Type	Operation	Location	RMS	Calibr.	Time base	Safety
1	Stationary	1972	Poland,Borowce	1 meter	Permanent target	VHF	
2	Mobile	1973	Egypt,Helwan	-"-	-"-	Loran C	
3	Air transp.	1975	Bolivia,Patacamaya	-"-	-"-	VHF	
4	Stationary	1975	USSR,Crimea	-"-	-"-	Loran C Rubidium clock	
5	Stationary	1976	USSR,Zvenigorod			TV	
6	Stationary	1975	CSSR,Hradec Kralove	-"-	-"-	TV	
7	Air transp.	(1975)	CSSR,Prague			Cesium clock TV	
8	Stationary	1976	USSR,Crimea			TV	
9	Stationary	1976	India,Kavalure	-"-	-"-	Cesium clock Transit	
10	Stationary	1977	Cuba,Santiago de Cuba	-"-	-"-	Loran C	
11	Stationary	1977	Hungary,Penc	-"-	-"-	Transit	

Tab.2. Long Arc fit using |8| SAO Diferencial Orbital Improvement Program with abbruated gravity field.Residuals.System errors. (Adaptive threshold).

Station Helwan Year 1977,Month October

SAO day	No.of range obser.	Observ. reject by SAO	Range residuals /meter/	Standard deviation /meter/	Note
42339	21	1	from 382 to 297	0,63	Residual systematic Possibly timing problem
42340	61	9	from 375 to 184	0,35	atto
42341	15	1	-10.7 - 1.6	0.72	Data looks good
42342	14	0	-10.7 -12	1.01	atto
42342	52	4	-6.8 -9.7	0.46	atto
42343	25	1	-20 -15	0.54	atto
42344	91	15	-11 - 7	0.46	excellent
42346	50	5	0.2 13	0.42	nice pass

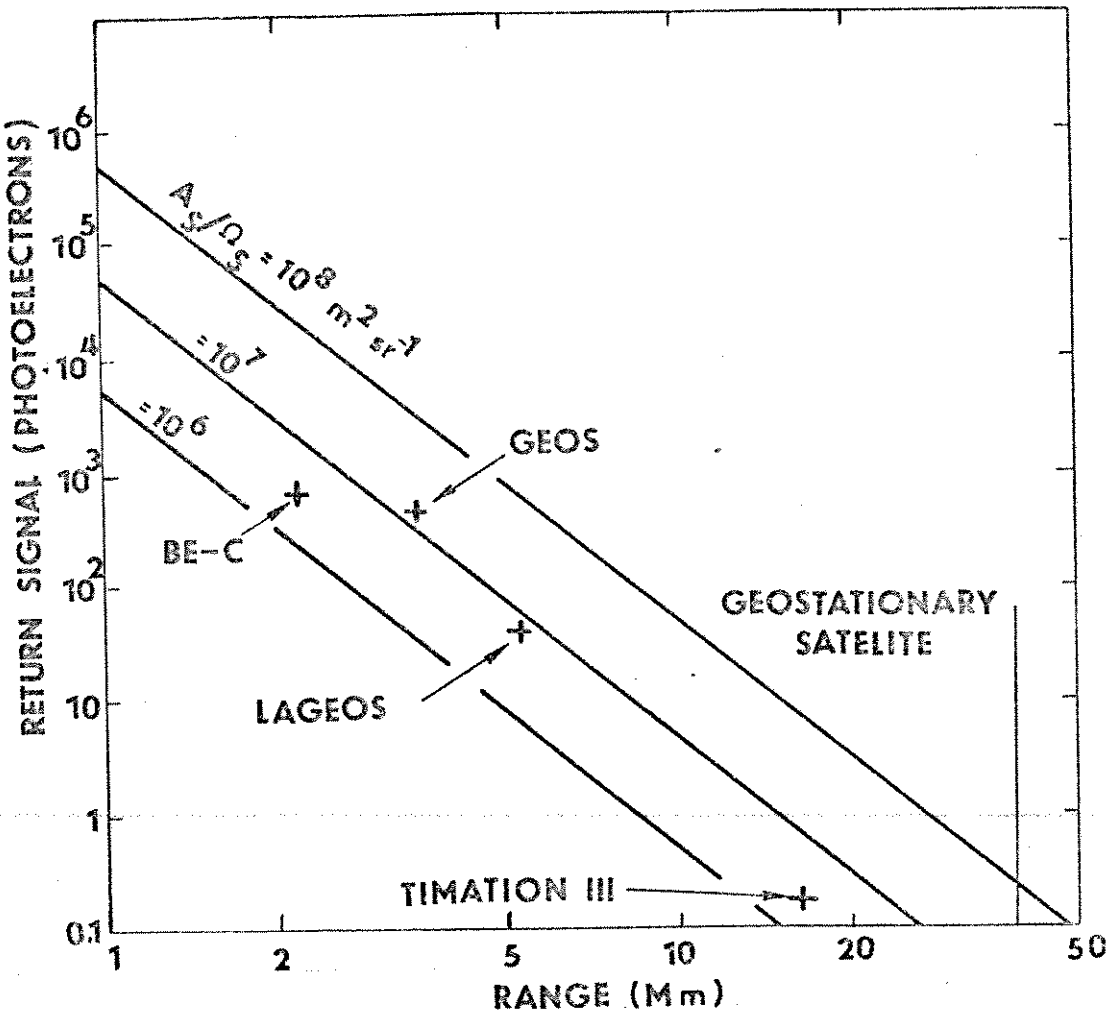

Characteristic of system	INTERKOSMOS laser radar
η_T, optical efficiency of the transmitting telescope	90%
E , laser energy	1 J
A_R, aperture area of the receiving telescope	0.07 m²
Θ_R, transmitter beam divergence	0.3 miliradians
T , one way atmospheric transmittance at 694 nm	58%
η_R, conversion efficiency of receiver incl.losses	1.5%
hν, energy of one photon at 694 nm	$2.86 .10^{-19}$ J

Fig.1

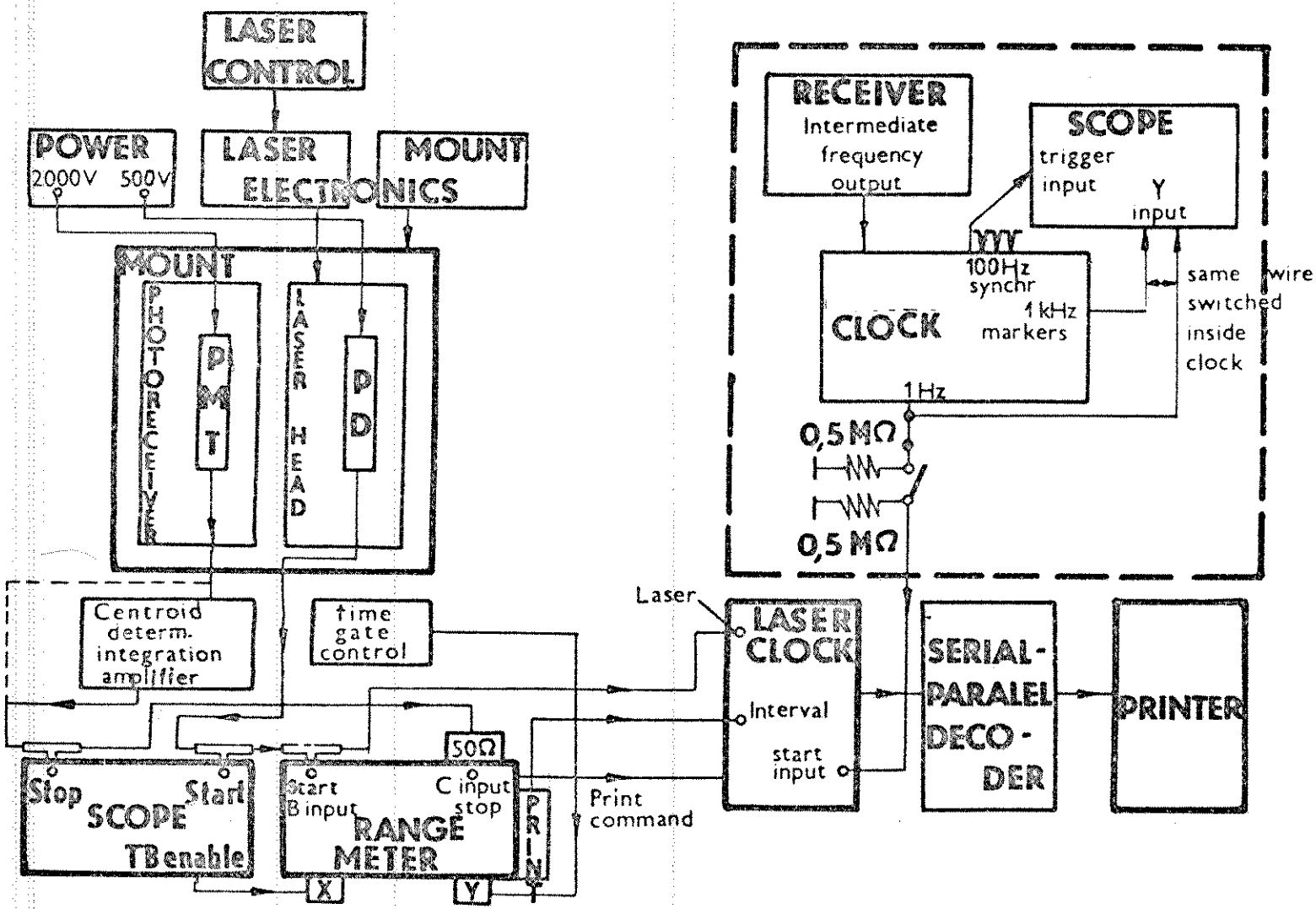
DISTANCE MEASUREMENT SCHEME.
LASER CONTROL
POWER
2000V 500V
LASER ELECTRONICS
MOUNT
MOUNT
PHOTORECEIVER
PMT
LASER HEAD
PD
RECEIVER
Intermediate frequency output
SCOPE
trigger input
Y input
100Hz synchr
1 kHz markers
CLOCK
1Hz
same wire switched inside clock
0,5MΩ
0,5MΩ
Centroid determ. integration amplifier
time gate control
Laser
LASER CLOCK
Interval
start input
SERIAL-PARALEL DECO-DER
PRINTER
50Ω
Stop
Start
SCOPE
TBenable
Start B input
C input stop
RANGE METER
X
Y
PRINT
Print command

Fig. 2


INTERKOSMOS LASER RADAR NETWORK.
POLAND
ZVENIGOROD
USSR
CSSR
CRIMEA
HUNGARY
SANTIAGO
CUBA
CAIRO
EGYPT
NAVALUR
INDIA
LA PAZ
BOLIVIA

Fig. 3

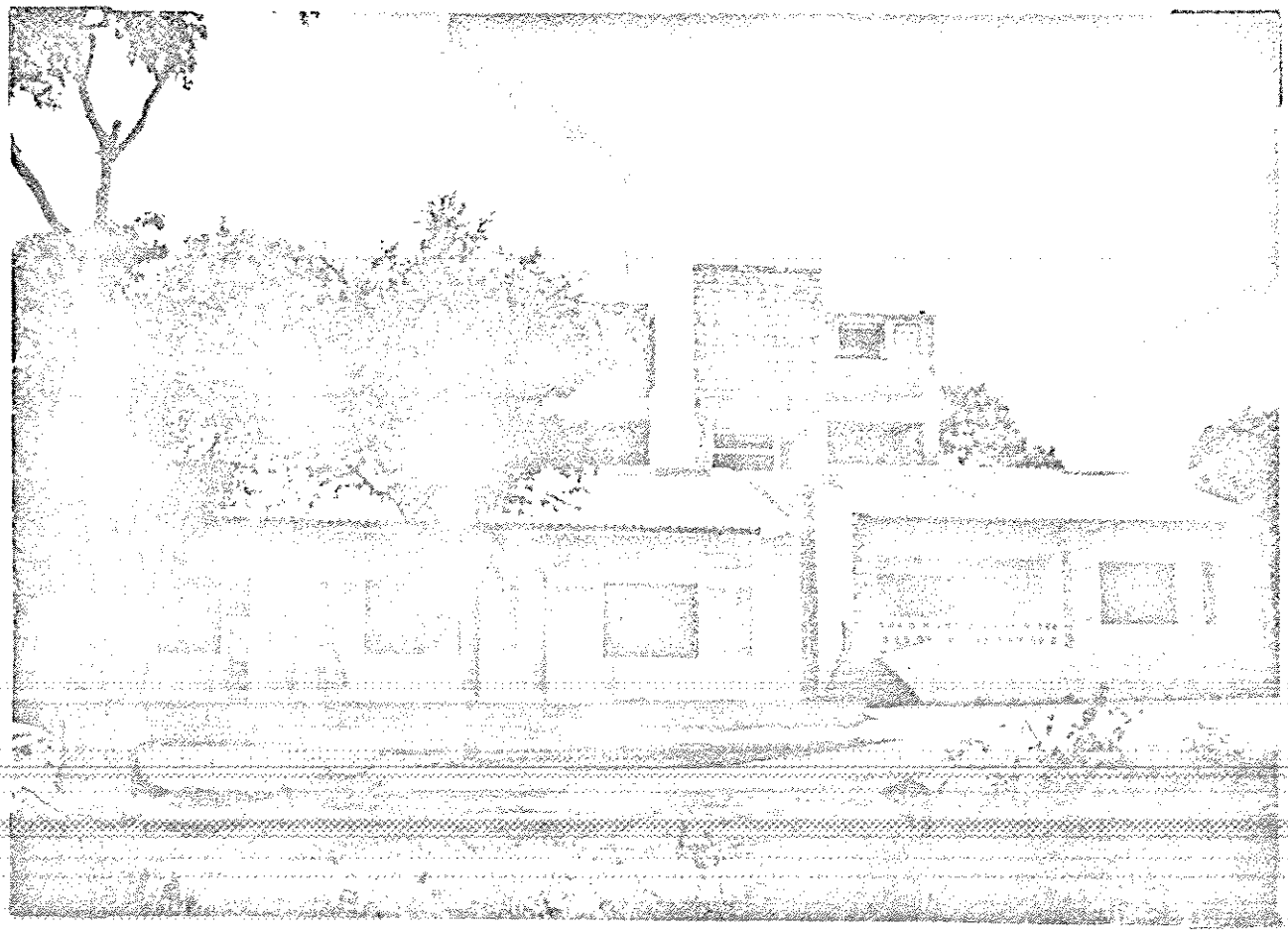

Fig. 4

THE SMITHSONIAN ASTROPHYSICAL OBSERVATORY SATELLITE RANGING HARDWARE

M. R. Pearlman, N. W. Lanham, J. Wohn, J. M. Thorp,
E. Imbier, and F. D. Young

Smithsonian Astrophysical Observatory
Cambridge, MA

INTRODUCTION

The Smithsonian Astrophysical Observatory (SAO) operates four satellite ranging laser systems to support research in geodesy and geophysics. The systems — in Natal, Brazil; Arequipa, Peru; Orroral Valley, Australia; and Mt. Hopkins, Arizona — have been in routine operation for 8 years. During the last 3 years, the lasers have been equipped with pulse-processing systems and minicomputer control and data-processing systems. Work has also been under way to install pulse choppers in the systems to reduce the laser pulse width.

The SAO laser ranging system shown in Figure 1 has a static pointing mount that is aimed by means of computed predictions of satellite azimuth and altitude. The predictions are computed and fed to the mount by minicomputer, which also collects and preprocesses the laser data on line. The system operates in both day and night conditions.

LASER TRANSMITTER

The laser, a ruby system built in an oscillator-amplifier configuration, generates an output of 5 to 7 joules in a 25-nsec pulse (half-power, full width). The system uses a Pockels cell and a Brewster stack for a Q-switch and operates at 8 pulses per minute. Both the 0.95-cm (3/8-inch) diameter oscillator ruby rod and the 1.6-cm (5/8-inch) diameter amplifier ruby rod are mounted in 15.2-cm (6-inch) double elliptical cavities, each containing two linear flashlamps. The optical cavity of the oscillator is formed by a flat rear mirror, with a reflectivity of 99.9%, and the uncoated front of the oscillator rod.

This work was supported in part by Grant NGR 09-015-002 from the National Aeronautics and Space Administration.

The oscillator output of 1 to 2 joules is coupled into the amplifier through a beam-expanding telescope. The amplifier has a single-pass gain of about 5. Both ends of the amplifier rod are antireflective-coated. The amplifier output is expanded to a diameter of 7 cm and passes through the 12.7-cm (5-inch) objective lens of a Galilean telescope. The diameter of the output-beam divergence can be adjusted from 0.5 to 5.0 mrad. Mounted at the output of the laser, photodiodes pick up atmospherically scattered light from the outgoing pulse and send an electrical start signal to the ranging system electronics. This basic laser transmitter has been in use in our network since 1969. Additional details on these lasers are given in Pearlman et al. (1973, 1975).

During the past 3 years, SAO has made several attempts to improve range accuracy by reducing the laser output pulse width with a chopper. The early versions of this system, based on a laser-triggered spark gap, proved to be too sensitive for our operational environment and could not be made to operate in a routine, reliable manner. To overcome this problem, SAO and Lasermetrics, of Teaneck, New Jersey, have designed an electronically triggered system that is now being tested at Mt. Hopkins. Additional units are being built for the other three stations. A diagram of the chopper is shown in Figure 2.

The chopper is basically a krytron-activated Pockels cell with appropriate polarizers for the necessary transmissions and isolation. A Blumlein circuit provides the proper high-voltage pulse to operate the Pockels cell, and a PIN diode and avalanche transistor circuit to trigger the system. The Blumlein is essentially a delay-line structure, in which delays and reflections are used to produce a high-voltage rectangular pulse of desired width from a voltage step provided by the krytron. The pulse width is adjustable by the length of the Blumlein. The present configuration utilizes a ceramic Blumlein with a length of 15 cm, a width of 1.75 cm, and a dielectric constant E = 30; this system produces a 6-nsec-wide output pulse with a 1-nsec risetime.

The optical assembly of the chopper has been designed to fit between the present laser oscillator and amplifier sections, thus minimizing installation impact in the field. The assembly consists of a thin-film dielectric polarizer sharpener and analyzer, a KDP* 50Ω Pockels cell, and a half-wave plate to match optical polarization to the laser amplifier. The Pockels cell is operated in a pulse-on for transmission mode. The pulse chopper timing is controlled in a gross sense by

optical attenuation in front of the PIN diode; fine tuning is made by threshold adjustments to the preamplifier.

The laser can be readily switched electronically from the Q-switched mode to the chopper mode. The laser produces about 1 joule in the 6-nsec chopper mode. In routine operation, the chopper will be used with most of the low orbiting satellites, while the Q-switched mode will be used with Lageos, NTS-2, and possibly some of the lower satellites with small effective cross sections.

RANGING SYSTEM ELECTRONICS

The ranging system electronics consist of a clock, a firing control, a range-gate control, a processing system for the start and stop (return) pulses, a time-interval unit, and a data-handling system, which feeds an on-line minicomputer. The clock, synchronized to within 1μ sec of each station's master clock, controls the firing rate and the time of the laser firing and provides the epoch of observation. Both the firing rate and the time of the laser firing can be controlled by the laser control unit. The firing time can be shifted manually by multiples of 0.001 sec, with a maximum of 3 sec, to account for the early or late arrival of a satellite at a predicted point in its orbit. The range-gate control unit, which provides a gate to the counter and the pulse-processing system, is normally operated with a 20-μsec window. The time-interval unit, with a resolution of 0.1 nsec, is triggered on and off by outputs from the pulse-processing system.

The pulse-processing system records the width and area of the outgoing laser pulses and the pulse shape of the returns. The range measurements are referred to pulse centers to avoid random and systematic errors due to pulse irregularities. The pulse processor is divided into two sections, the start and stop channels. The start channel is based on dual discriminators and pulse integrators to measure pulse width and area. The stop channel, which records return-pulse waveforms is basically a commercially available waveform digitizer and a time-interval unit. The digitizer has 20 sampling channels with spacing adjustable from 1 to 25 nsec. Q-switched operation uses 5-nsec spacing, while the chopper mode employs 1-nsec spacing. The pulse-processing system is discussed in more detail in Pearlman et al. (1975). A diagram of the system is shown in Fig. 3.

In operation, the laser output wave shape is recorded before each pass and then used in a cross-correlation analysis to determine the pulse centers. This requires, of course, that great care be taken to ensure that laser operating conditions (pulse shape) do not change appreciably during a pass.

MOUNT AND PHOTORECEIVER

The azimuth-altitude static-pointing mount has a pointing accuracy of better than ±30 arcsec. The system is driven by stepping motors in an open-loop mode, with the stepping-motor drive-system gears allowing for slewing speeds of 2°/sec and positioning increments of 0°.001. The mount has goniometers graduated to 0°.001 for reference and verification. Predictions, including pointing angles and range-gate settings, are entered in the system on a point-by-point real-time basis from the on-line minicomputers.

The receiving telescope is a 50.8-cm (20-inch) Cassegrain system with additional optics designed to focus an image of the primary mirror on the photocathode of the photomultiplier tube (PMT). The optics following the flat secondary mirror pass the collimated return signal to a 7 Å filter that is both tilt- and temperature-dependent. Effects of age and temperature are compensated for by means of a micrometer tilt adjustment that tunes the filter. Adjustable field stops and a provision to insert combinations of neutral-density filters are available.

The photodetector, an RCA 7265, was chosen for its quantum efficiency of 4% at 6943 Å. The PMT has a gain of 5×10^7 and a risetime of approximately 3 nsec as operated in the SAO system.

MINICOMPUTER AND CONTROL SYSTEM

The SAO laser stations have Data General Nova 1200 minicomputers for data processing and system control. Each minicomputer has 32K words of 16-bit core memory and a floating-point processor. Its peripherals include three block-addressable magnetic-tape units, alphanumeric CRT display units, a high-speed paper-tape reader and punch, and thermal printers with keyboards.

The minicomputers were originally installed at the laser sites for stand-alone operation in 1975. The direct connection with the lasers was undertaken over the past year. In connecting the minicomputers to the lasers, we looked for a scheme that would have minimum impact on the laser operation and existing hardware and software. We decided to build an interface that made the minicomputer emulate the original paper-tape input-output equipment in terms of electronic interaction and communication. To do this, the control pulses originally used to start the paper-tape reader and punch were adapted to cause hardware interrupts in the minicomputer. The interface was designed to distinguish between the interrupts (input or output) and to enable the software to perform the appropriate action, i.e., either put data on the laser systems by input lines or take data off by output lines. With the appropriate interrupt-driven software, this relatively simple system has fulfilled our needs for both interface and display. A diagram of the minicomputer system and interface is shown in Figure 4.

The minicomputer generates pointing predictions from orbital elements provided by Headquarters and feeds them to the laser in real time for pointing and range-gate adjustment. The minicomputer receives all incoming data on line from the laser system in real time and performs most of the preprocessing, including centroid determination, start-channel correction, and calibration. A second pass through the machine prepares the quick-look data message for transmission to SAO. The minicomputer provides detailed analysis of hardware (start and stop channel) and target calibrations as well as a review and summary of satellite and associated prepass and postpass calibration data on a pass-by-pass basis.

During ranging operations, the operator has a real-time display of point and pass parameters, including return-pulse shape, output-pulse parameters, range residuals to predictions, and data and hardware error diagnostics.

REFERENCES

Pearlman, M. R., Lehr, C. G., Lanham, N. W., and Wohn, J., 1975. The Smithsonian satellite ranging laser system. Presented at the General Assembly of the International Association of Geodesy, Grenoble, France, August.

Pearlman, M. R., Thorp, J. M., Tsiang, C. R. H., Arnold, D. A., Lehr, C. G., and Wohn, J., 1973. SAO network: Instrumentation and data reduction. In 1973 Smithsonian Standard Earth (III), ed. by E. M. Gaposchkin, Smithsonian Astrophys. Obs. Spec. Rep. No. 353, pp. 13-84.

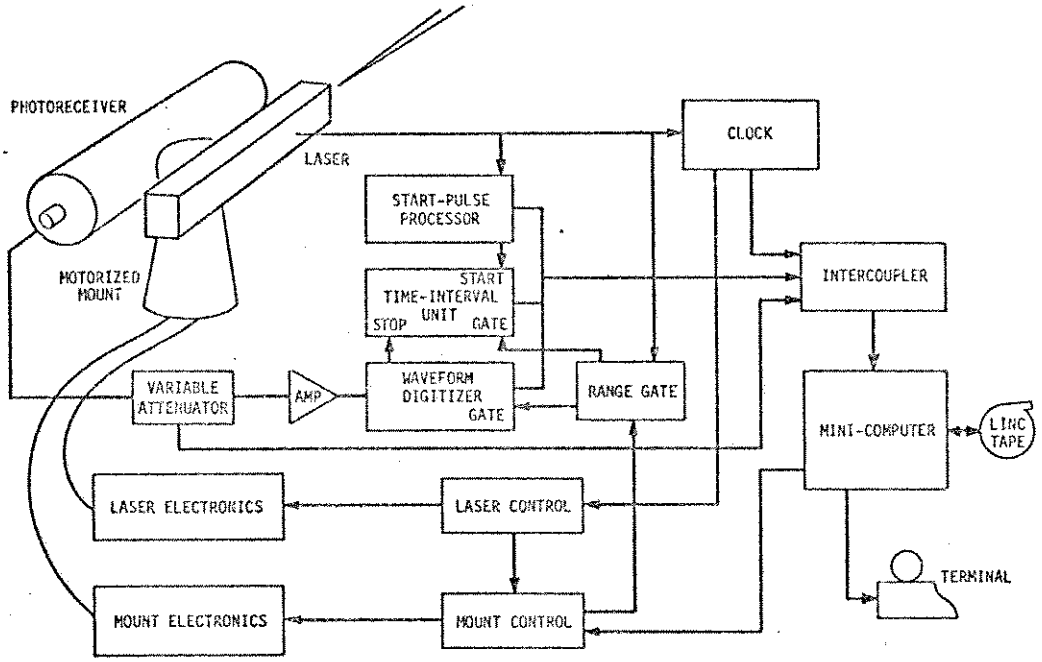

Figure 1. Block diagram of the laser system.

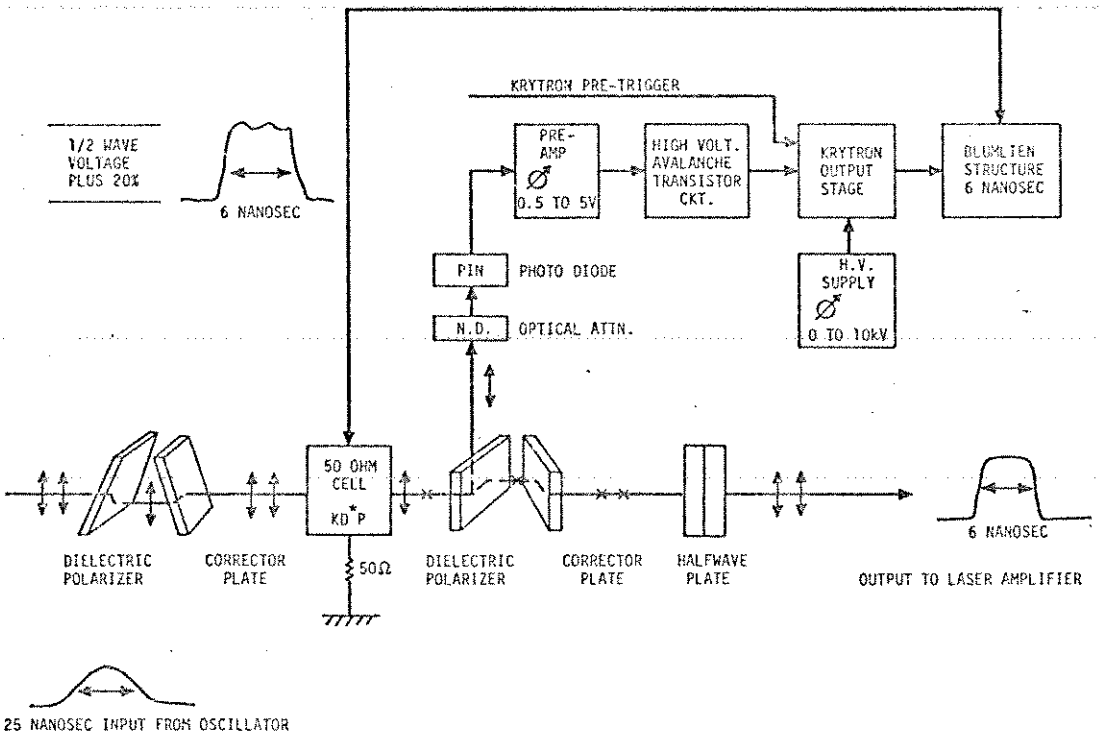

Figure 2. Krytron activated pulse-shaping system.

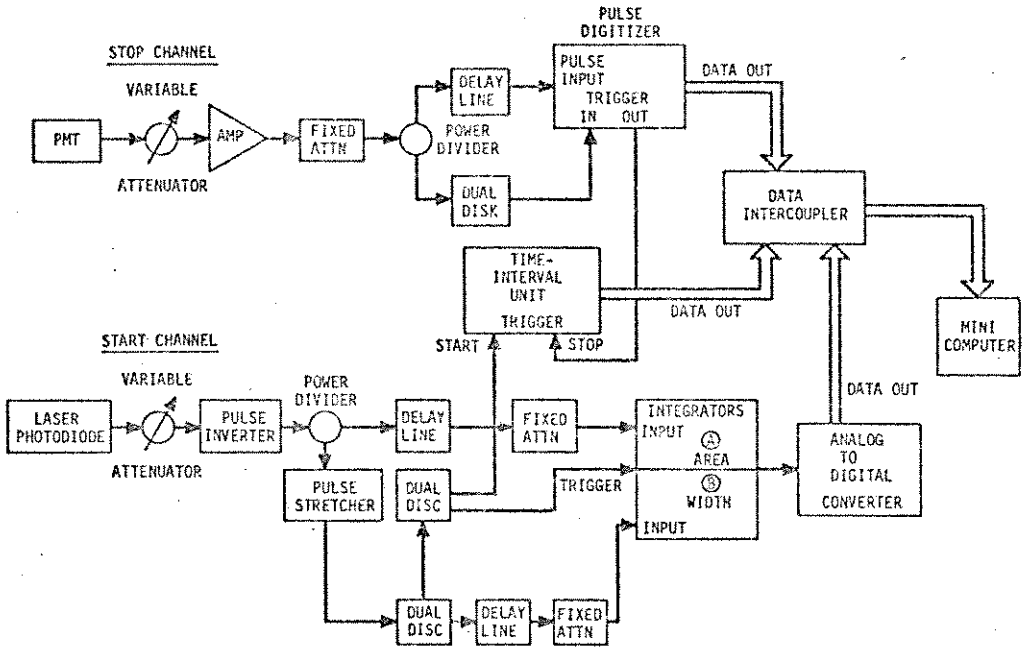

Figure 3. Pulse-processing system.

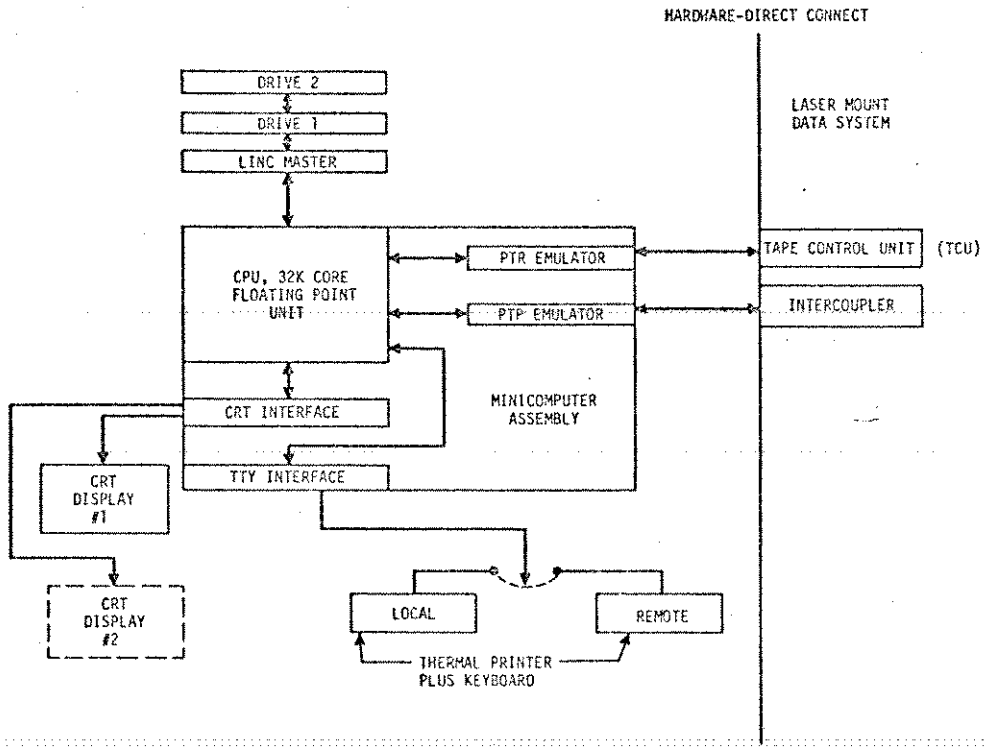

Figure 4. Minicomputer control system.

THE SATELLITE RANGING SYSTEM AT KOOTWIJK

L.Aardoom , F.W.Zeeman
Delft University of Technology, Delft (The Netherlands)

INTRODUCTION

At the observatory for satellite geodesy near Kootwijk - lat. 52° 10' N long. 5° 48' E - the Geodetic Institute of the Delft University of Technology operates a laser ranging system since August 1976.
Routine day and night operation is possible on all cooperative geodetic satellites presently in orbit, with the exception of daytime operation on LAGEOS. Modification of the system in order to decrease the minimum signal-to-noise ratio for daytime tracking is in preparation.
The measurements so far show an accuracy level of 15 - 30 cm (r.m.s.) in satellite ranging and 3 - 6 cm on ground targets up till 1 km.
Accuracy will be improved using waveform analysis.

LASER SYSTEM

The ruby pulse laser system consists of a multi-mode Q-switched oscillator, a spark-gap activated pulse chopper and two amplifier stages. It can produce 4 ns wide pulses at a maximum rate of 15 ppm. The output energy in routine operation is 1 - 2 Joule (3 Joule max.). A sketch of the configuration of the oscillator, the pulse chopper and the alignment optics is given in figure 1.
The laser has been installed on an optical bench in an air-conditioned room to avoid any problems with moisture, dust and stability of alignment.

TRANSMITTING AND RECEIVING TELESCOPE

The transmitting telescope is of a refractive coudé design and the receiving telescope is of a partial coudé design (optical path passes through the elevation axis only) with a catadioptric (lens - mirror) optical train.
The transmitting telescope is located where the second reflector is usually positioned in the more conventional cassegrain reflecting telescope. By doing so the size of the complete optical system has been significantly

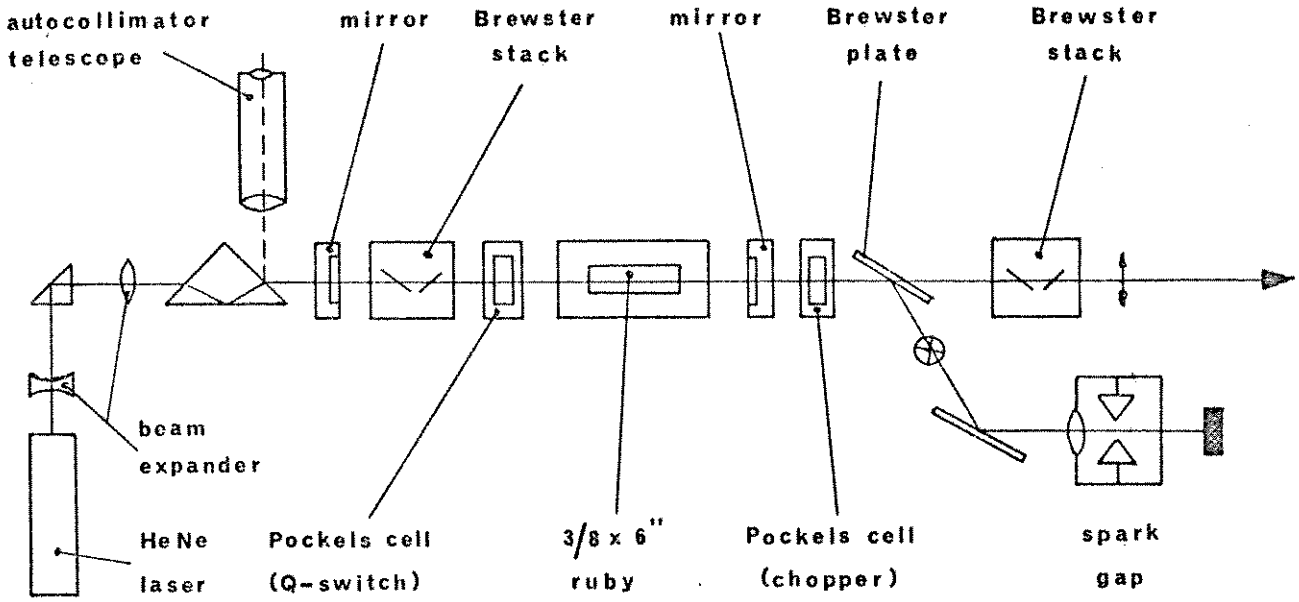

Figure 1

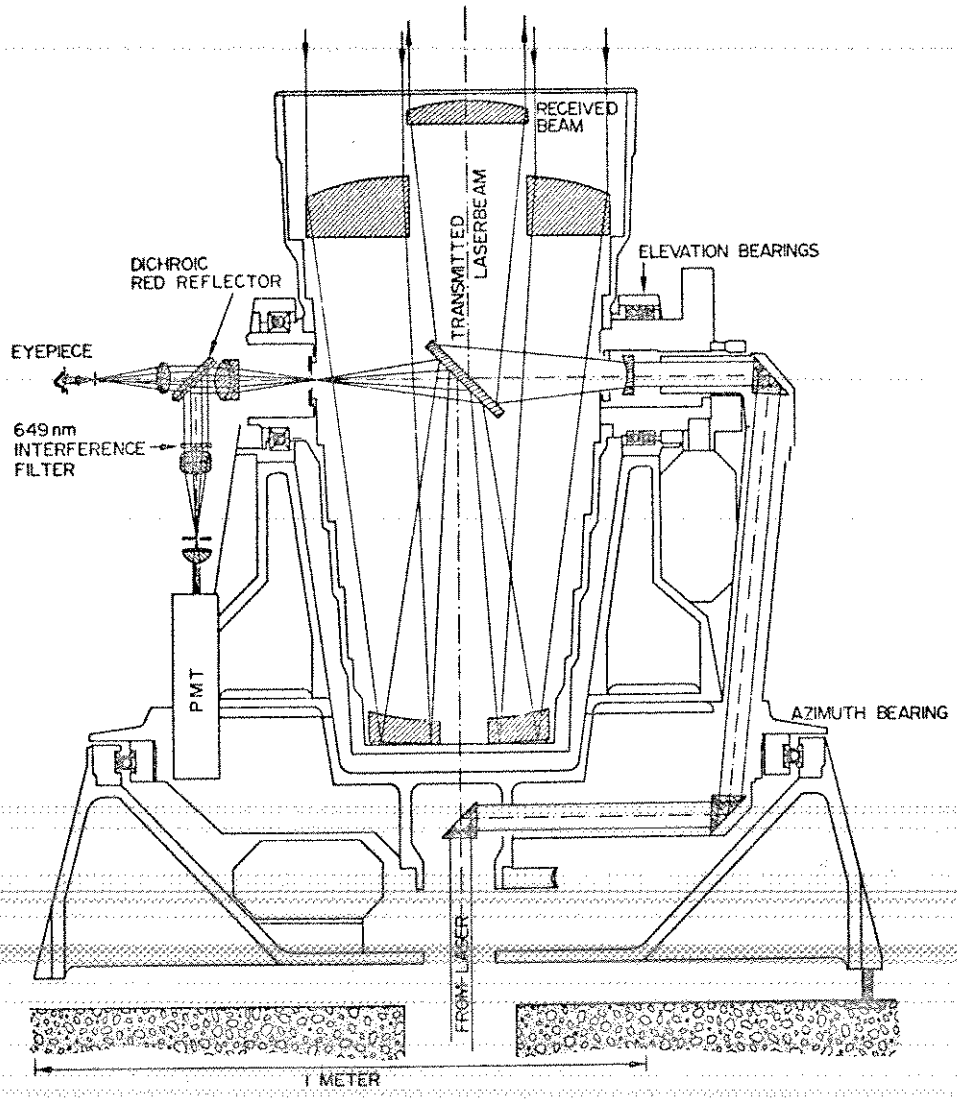

Fig. 2. Coudé telescope.

reduced (figure 2.).

The transmitted laser beam has a diameter of 19 cm and the divergence is adjustable from 1 to 20 arcminutes.

The aperture of the receiving telescope is 50 cm and the field of view is adjustable from 1 to 20 arcminutes.

The mount's angular position is read out using fine and coarse absolute optical shaft encoders. The mount control unit then compares the actual position with the desired position. The error signal generated is used to drive the DC servo motors. The absolute pointing error of the mount is less than 20 arcseconds. The total positioning range of the elevation axis is 0 - 180° ; the range of the azimuth axis is 0 - 720°.

By means of a dichroic red reflector the received light is split into wavelengths $>$ 6500 Å which are directed to the photomultiplier and wavelengths $<$ 6500 Å going to an eyepiece. In this way the operator can see sunlit satellites to a visual magnitude of + 13. This feature has shown to be extremely useful in acquiring poorly predicted satellites with a narrow beam.

The reflection of the transmitted laser beam on the second prism has been directed via a secondary optical path (not shown in figure 2) and an adjustable attenuator to the photodetector. In this way it is possible to perform system calibrations without an external target.

MEASURING SYSTEM

The detection circuitry and time interval meter is composed of the following principal equipment:

- photomultiplier: RCA model 8852
- interference filters: bandwidths 3 Å and 10 Å
- preamplifier: Hewlett Packard model 10855A, ampl. 24 dB, 1300 Mhz, noise figure 8 dB

xx - preamplifier: Trontech W 500 B, ampl. 31 dB, 500 MHz, noise fig. 1.5 dB

- progr. attenuator: Texcan PA - 51 , atten. 0 - 63 dB
- amplifier: Avantek AV - 9T , ampl. 30 dB, risetime 0.8 ns

xx - amplifier: Trontech W 500 C, ampl. 40 dB, 500 MHz

- range gate generator: SAO design, window 1 - 99 μs, range 1 - 999999 μs
- time interval counter: Hewlett Packard 5360A , H01 - 5379A , resolution 0.1 ns , discrimination technique: fixed level, leading edge
- start pulse detector: ITT F-4000 biplanar photodiode, risetime 0.5 ns

xx - discriminator start pulse: Ortec 473A constant fraction discriminator

xx - discriminator stop pulse: EG & G T 105/ N leading edge discriminator

- waveform digitizer: Tektronix R 7912 transient digitizer, package WP 2003, to be linked to a Hewlett Packard 21 MX-E minicomputer (second half 1978)
- epoch clock: SAO design, resolution 1 μs

The xx marked instruments have been integrated in the system recently (May 1978).

CALIBRATION PROCEDURE

Before and after each satellite pass a minimum of 10 calibration measurements are carried out, using the internal short circuit light path. This light path has been measured with an AGA 700 laser geodimeter to a preliminary accuracy of 3 cm.

During the measurements the transmitted beam is attenuated by a factor of about 10^6. On the photomultiplier side an optical attenuation is introduced in order to equalize the calibration return signal with the average return signal from the satellite.

STATION TIMING

Standard frequency and station time is derived from a rubidium standard. The principal synchronisation technique is time comparison against the Netherlands national time standard UTC_{vsl} in The Hague using television broadcast synchronisation pulses.

Present overall timing accuracy: 1 microsecond UTC.

LASER SAFETY

The following safety measures have been taken:

- personal protection: safety goggles, warning signs, optical and electrical shielding, etc.
- careful control system design, including strict operating procedures
- attenuation of the laser beam when performing tests and calibration measurements
- airtraffic protection: an optical airplane detection system with automatic laser inhibiting.

PREPROCESSING

All satellite observations are subjected to an adjustment with respect to a best fitting elliptical orbit, in order to have a first insight into the number of likely succesful returns. After rejecting probable outliers each residual is individually tested statistically with respect to an a priori estimated single shot precision of 1.5 ns (round travel time). Figure 3 gives an example of the residuals of a typical LAGEOS pass.
As mentioned already pre- and post-pass calibrations are carried out routinely. These measurements are used to update the value of the system delay with respect to the reference point at the intersection of the two telescope axes.

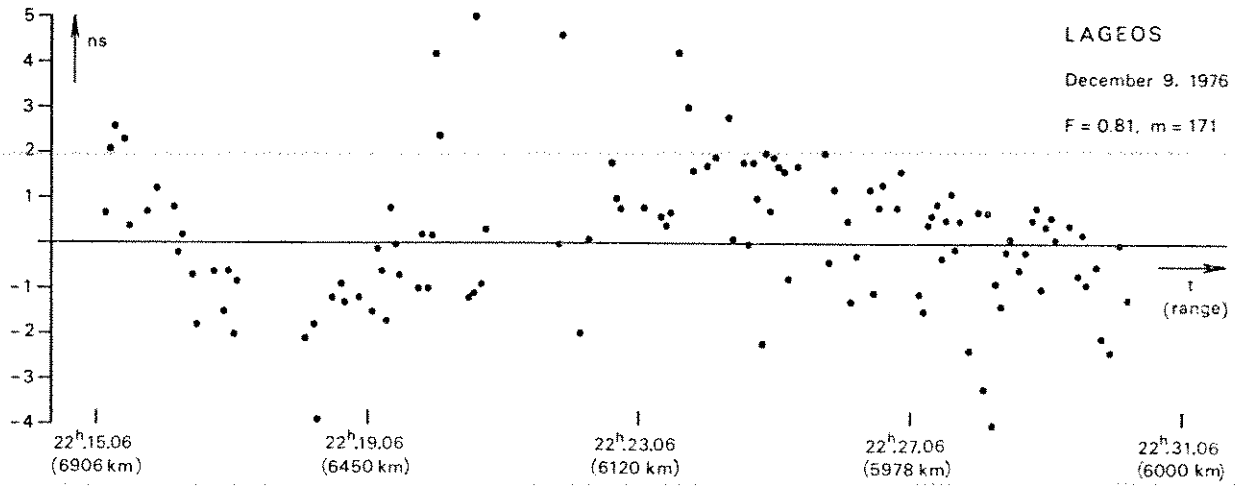

fig. 3

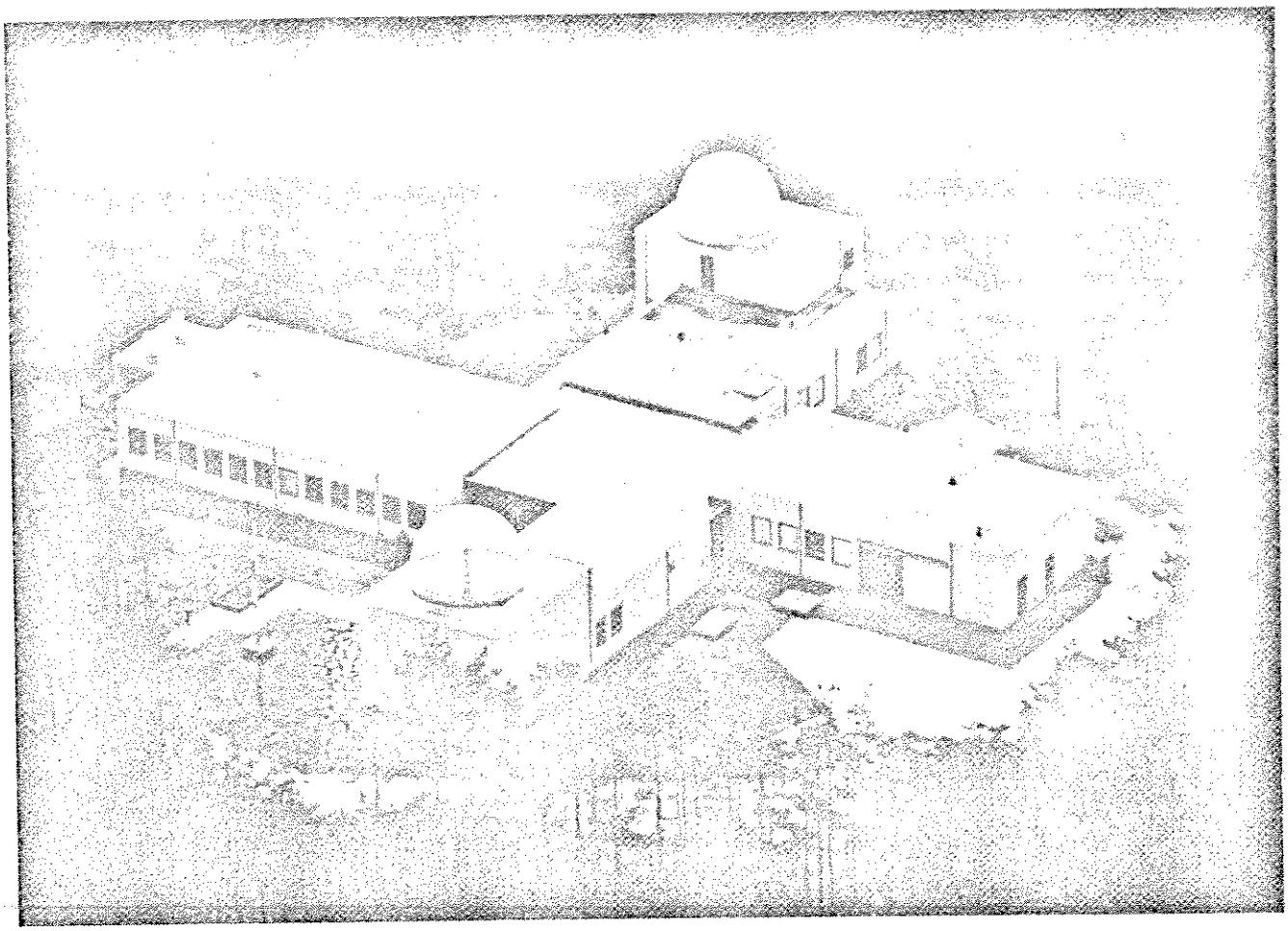

KOOTWIJK OBSERVATORY

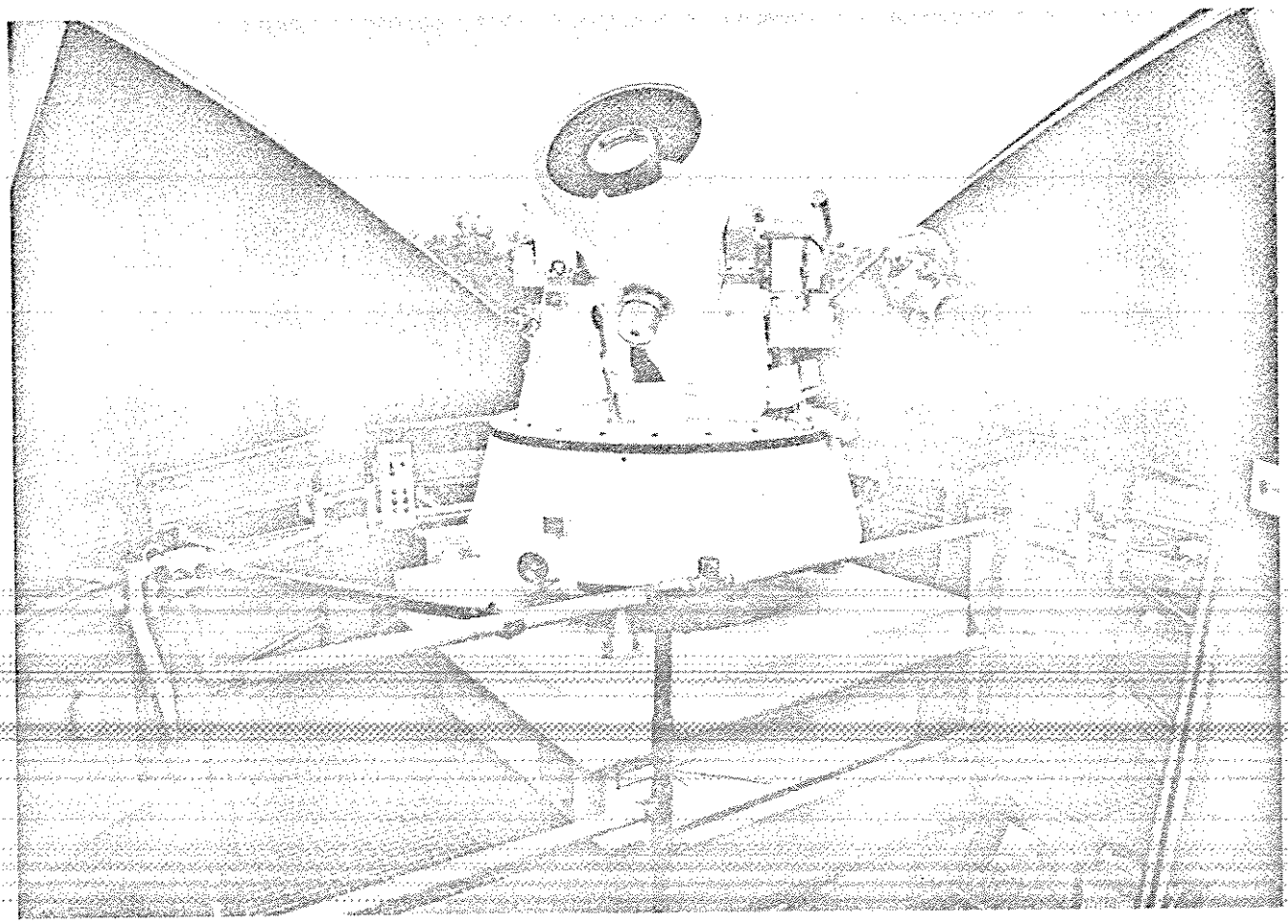

COUDÉ MOUNT

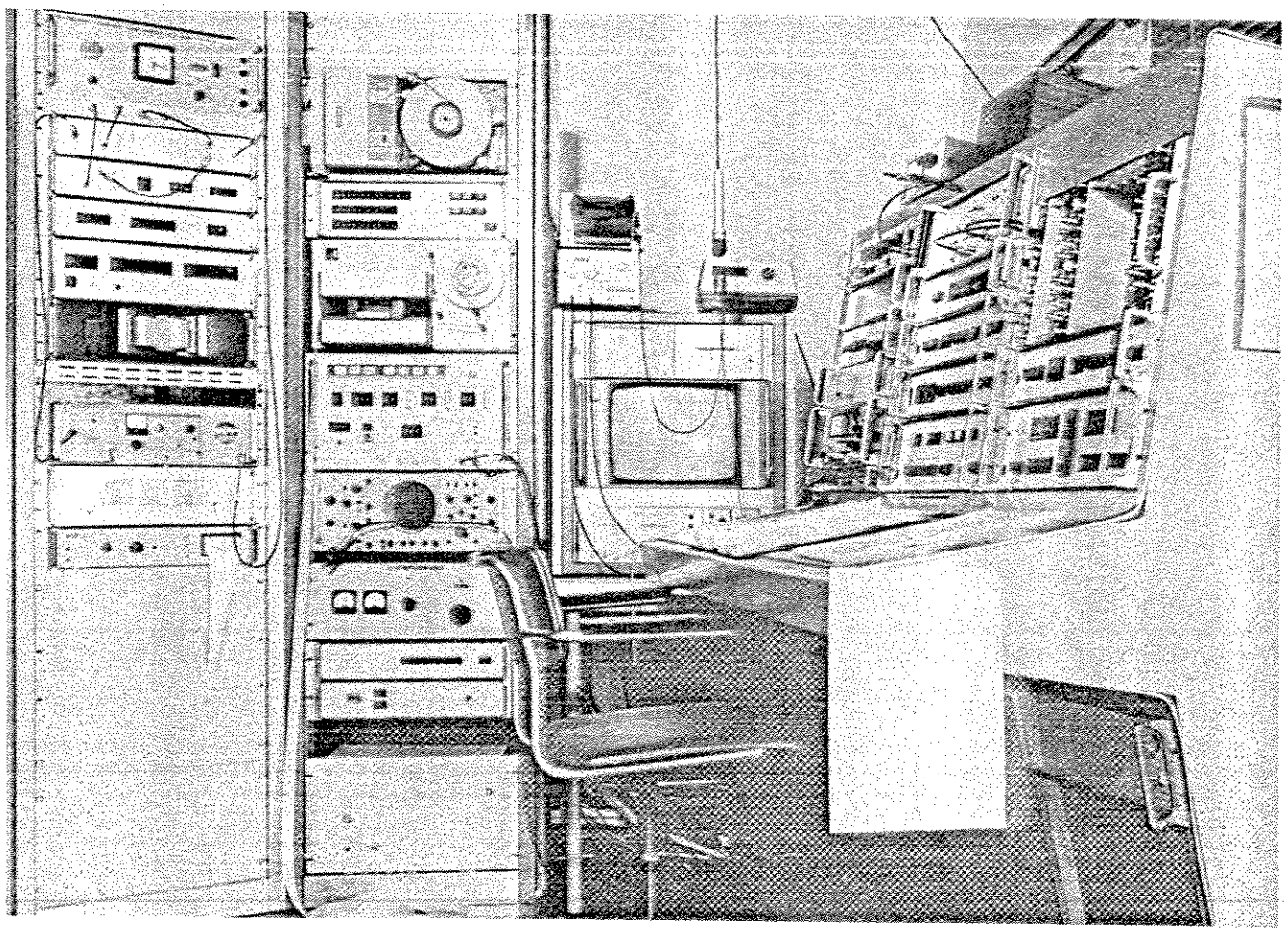

CONTROL ROOM

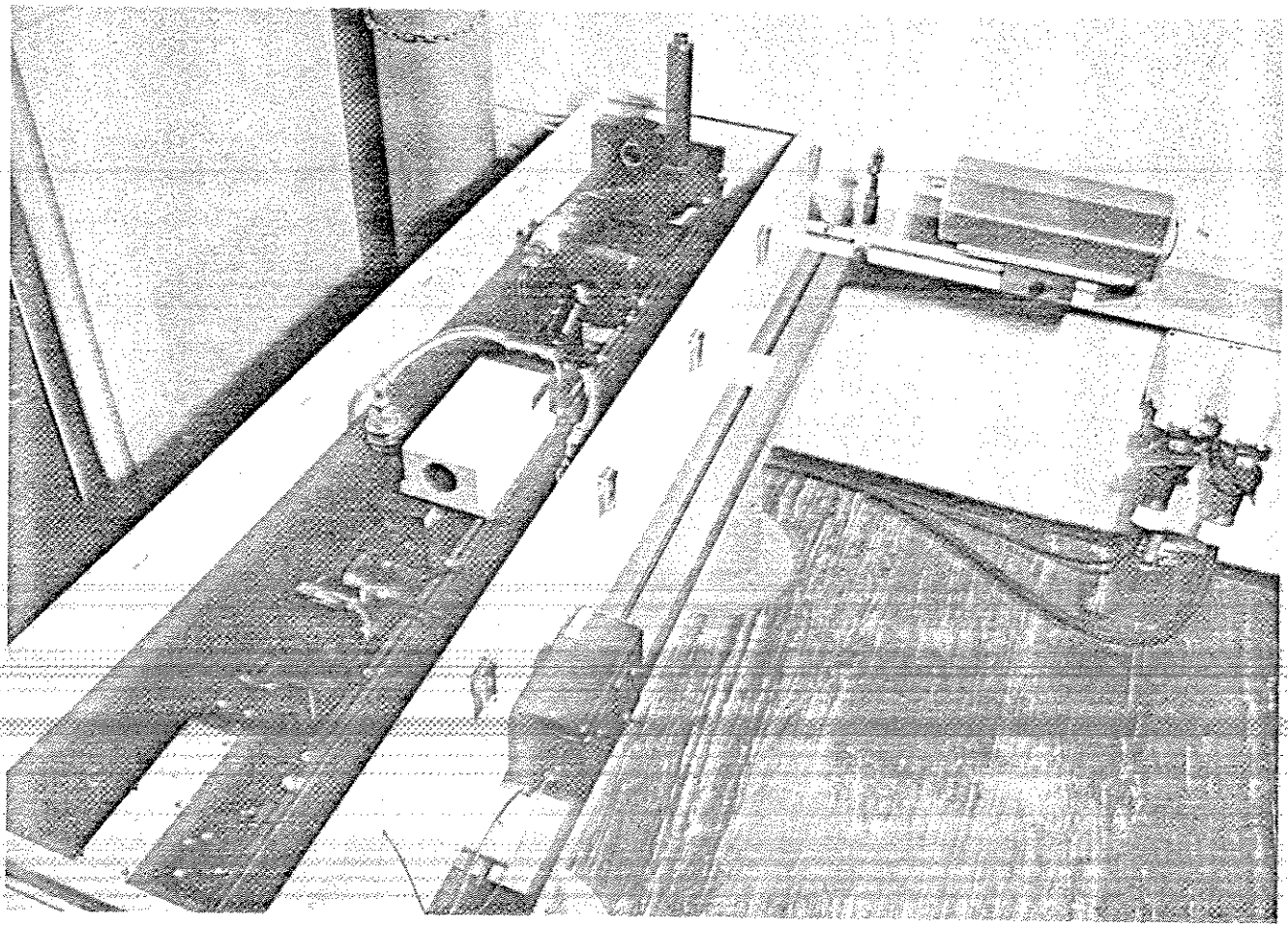

LASER OSCILLATOR

SUMMARY STATISTICS STATION: 7833 KOTWIK PERIOD: 1976-1978 (DATE: 780516 CODE: 01)

	CALIBRAT. (0000000)		BEACON-C (6503201)		GEOS-1 (6508901)		GEOS-2 (6800201)		STARLETTE (7501001)		GEOS-3 (7502701)		LAGEOS (7603901)		TOTAL	
	OBS	PAS	OBS	PAS	OBS	PAS	OBS	PAS	OBS	PAS	OBS	PAS	OBS	PAS	OBS	PAS
JAN	0	0	0	0	0	0	0	0	53	6	167	7	439	7	659	20
FEB	0	0	0	0	0	0	0	0	0	5	35	13	21	6	56	24
MAR	0	0	0	1	1132	21	0	0	165	21	252	18	560	13	2109	74
APR	0	0	0	0	690	11	0	0	848	42	710	31	1359	15	3607	99
MAY	0	0	85	3	285	9	0	0	287	21	378	20	1138	7	2173	60
JUN	0	0	0	0	0	0	0	0	0	0	0	0	0	0	0	0
JUL	0	1	0	0	0	0	70	1	0	0	145	3	0	0	215	5
AUG	0	0	0	0	841	7	167	3	91	17	446	27	83	1	1628	55
SEP	0	0	0	0	358	4	144	3	659	42	787	30	153	9	2101	88
OCT	0	0	0	0	48	1	52	1	222	25	375	38	399	12	1096	77
NOV	0	0	0	0	0	0	101	1	466	40	533	26	884	17	1984	84
DEC	0	0	0	0	236	5	0	0	289	13	241	10	861	10	1627	38
TOT	0	1	85	4	3590	58	534	9	3080	232	4069	223	5897	97	17255	624

SATELLITE LASER RANGING INSTRUMENTATION AT THE POTSDAM STATION [1)]

Harald Fischer and Reinhart Neubert
Zentralinstitut für Physik der Erde
Potsdam, DDR

INTRODUCTION

The Potsdam laser ranging instrument is based on the satellite camera SBG made by Zeiss Jena, which was already in operation at the beginning of our laser work. The modification of the camera was done in such a way, that both photographic and laser observations are possible with quick switchover between the two modes of operation.

Tab. 1.: Specifications

Transmitter	
Laser energy:	1 ... 2 J
Pulse width:	15 ... 25 ns
Beam divergence:	1 ... 10 min of arc
Receiver	
Effective aperture:	320 mm dia
Field of view	1 ... 10 min of arc
Filter passband:	1 nm, T > 50 %
Photomultiplier type:	RCA C 31034 A
Resolution of time interval counter:	10 ns

According to the main data (see Tab. 1.) the instrument belongs to the first generation characterised by accuracies of about 1 m. The laser modification was put into experimental operation at the beginning of 1974.

1) Paper read by K. Hamal Additional information is contained in unread papers distributed to participants of the workshop.

Since that time more than 1000 points have been collected mainly from GEOS-satellites, but some from STARLET and LAGEOS too. The number of measurements may be increased by operating the instrument more routinely and by the planned modification for daylight tracking. In the following we give a short description of the instrument.

SYSTEM DESCRIPTION

The Potsdam laser ranging system is of almost conventional design and the diagrams of figure 1 and 2 are thought to be quite self-explanatory. We note here that both the start and stop channel contain constant fraction discriminators of identical characteristics. The epoch timer is initiated from the same pulse which starts the range counter. This is necessary to eliminate the time jitter of the passive Q-switched laser. To protect the sensitive GaAs-cathode photomultiplier, pulsed supply voltage is used. The output data are printed and punched on paper tape.

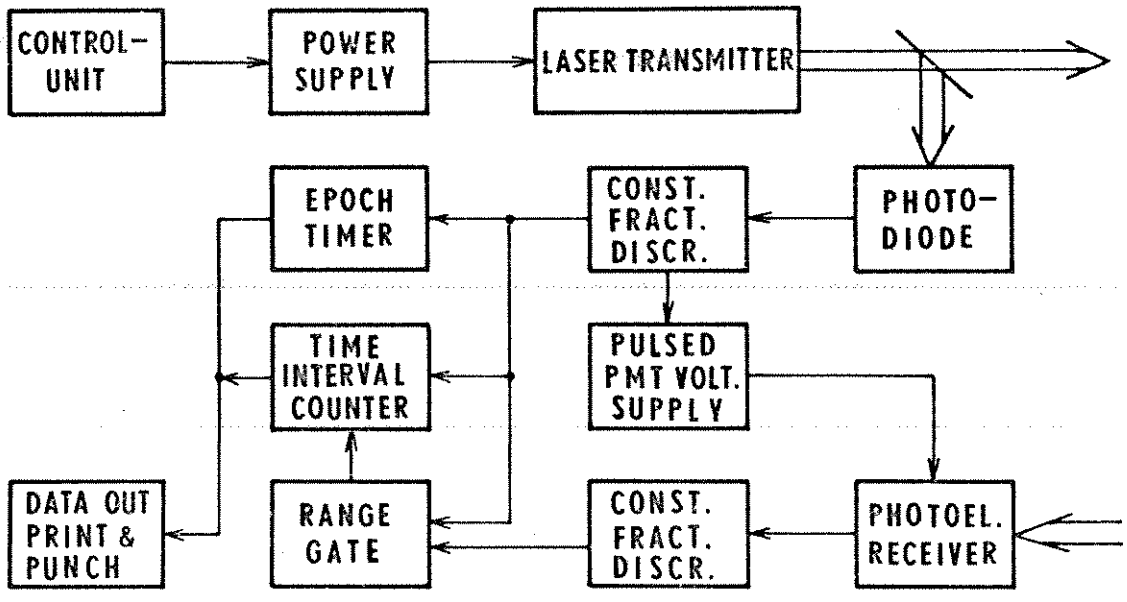

Fig. 1.: Block Diagram of the Laser Ranging System

1. Laser Transmitter

The laser used is a two-stage ruby system, which was constructed in our laboratory. The oscillator is Q-switched by the simple saturable dye method, giving pulses of 15 to 25 nanoseconds duration and energies of 0.3 to 0.5 Joule. After passing through the amplifier rod, the pulses have an energy of about 2 J. Both ruby rods are pumped by two linear flashlamps in diffuse reflection cavities. The repetition frequency is determined by the power supplies to 0.2 cps maximum. Using high stability charging units for the condenser batteries the reproducibility of the laser pulses has been found to be quite satisfactory. The Q-switching solution has to be exchanged after about 1000 shots.

2. Mount and Receiver Optics

The SBG-camera has a 4-axis mount which is well suited to visual tracking but the original tracking system is not sufficiently accurate for automatic operation. We have attached to the mount a theodolite for exact setting of the inclination of the 3^{rd} axis and digital encoders to the 3^{rd} and 4^{th} axis. This way an absolute pointing accuracy of better than 1 min of arc has been reached as checked by reference stars /1/. The Schmidt telescope of the SBG has been equpped with a hinged Cassegrain mirror which may be swept into the ray path in front of the photoplate assembly (figure 2). The switchover between photographic and ranging mode takes about one second. The photoelectric receiver package is placed behind the main mirror. It consists of the iris field stop, the temperature controlled filter unit, the photomultiplier and two bending mirrors. In 1976, the first bending mirror has been replaced by a dichroic one so that by an additional eyepiece the main telescope may be used as a guide too. this low cost improvement enabled us to track STARLET and LAGEOS visually.

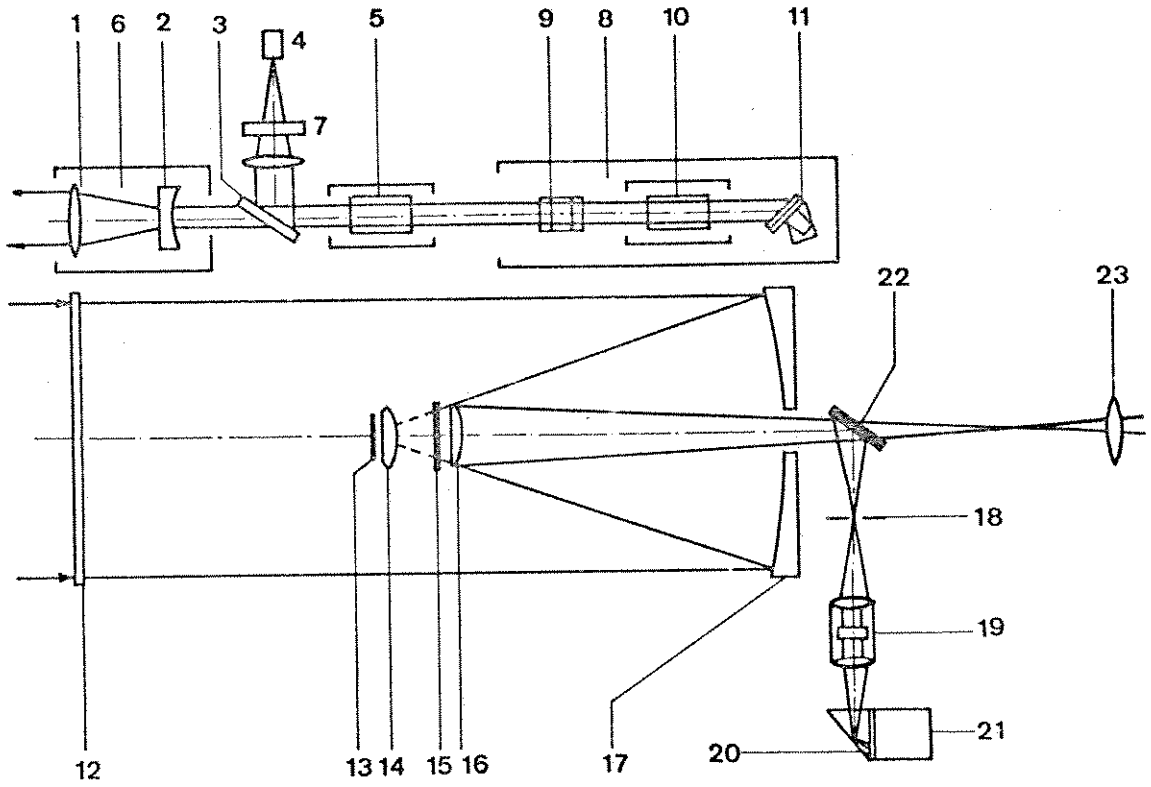

Fig. 2.: Optical Diagram of the Transmitter and Receiver System

1 = Objective Lens, 2 = Negative Lens, 3 = Parallel Plate, 4 = Silicon Photodiode, 5 = Amplifier Ruby, 6 = Beam Expander, 7 = Neutral Density Filter, 8 = Oscillator Stage, 9 = Etalon Reflector, 10 = Oscillator Ruby, 11 = Q-Switching Cell and Prism Reflector, 12 = Schmidt Plate, 13 = Photographic Plate, 14 = Field Flattening Lens, 15 = Shutter, 16 = Hinged Cassegrain Mirror, 17 = Main Mirror, 18 = Field Stop, 19 = Interference Filter, 20 = Prism, 21 = Photomultiplier, 22 = Dichroic Mirror, 23 = Eyepiece.

3. Receiver Electronics

Since 1977 we have used a RCA C 31034 photomultiplier. The measured quantum efficiency of about 20 per cent and the dark pulse characteristics let us expect a sensitivity enhancement of about 20 times compared to the former used C 31000. This was confirmed by calibration target measurements and by successful LAGEOS tracking.

Unfortunately the C 31034 has to be operated at anode currents below 10^{-7} A for a 30 s averaging time according to the manufacturer. To guarantee this the PMT supply voltage is held at 800 V dc and switched to operating voltage of 1600 to 1800 V for some milliseconds during possible echo return. In addition a safety circuit switches off the PMT voltage if the anode dc current exeeds 10^{-7} A.

The constant fraction discriminator is of the short circuited cable reflection, zero crossing type. The superposition of the signal pulse with reflected delayed pulse of opposite polarity has a zero crossing point which is almost independent of signal amplitude /2/. A tunnel diode trigger is used as zero crossing detector.

OPERATIONAL RESULTS

Laser tracking results obtained using visual guiding are quite satisfactory. For GEOS-satellites a data rate up to the maximum, determined by laser repetition frequency has been obtained. The possibility of alternating laser and photographic observations during one passage has been verified many times. In this case the time lost for laser tracking is about 20 sec for each plate depending on satellite height. A good test of sensitivity to date is the possibility to get echoes from the newer satellites STARLET and LAGEOS. Using visual tracking we got echoes from both satellites, but LAGEOS has been found to be very close to the sensitivity limit. Table 2 shows the printout of LAGEOS measurements of September 26th, 1977. The laser energy was 0.8 J and the divergence angle 1 min of arc. The receiver trigger level was set to 2 to 3 photoelectrons leading to an overall return rate of about 20 per cent.

Tab. 2.: Printout of LAGEOS-Measurement

STATION NO.: 1181 SATELLITE NO.: 7603901
DATE.: 1977 9 26

NO	EPOCH			DISTANCE	DEV.FROM PRED.
	H	M	S	MEGAM.	KM
1	3	32	49.8073	6.2739135	-4.10
2	3	34	54.2709	6.1509417	-4.37
3	3	35	27.1611	6.1261924	-4.42
4	3	37	7.8637	6.0713424	-4.54
5	3	37	21.3421	6.0664348	-4.54
6	3	37	42.7388	6.0598334	-4.56
7	3	37	54.9485	6.0567290	-4.57
8	3	40	40.2293	6.0619274	-4.55
9	3	41	4.2506	6.0700023	-4.52
10	3	41	40.3580	6.0856035	-4.48
11	3	42	35.3354	6.1172631	-4.40
12	3	44	44.6120	6.2283076	-4.14

References

/1/ FISCHER, H.; NEUBERT, R.: In: "Arbeiten zur Satelliten-geodäsie". Veröffentlichung d. Zentralinstituts f. Physik der Erde, Nr. 40, Potsdam 1976, S. 77-95

/2/ MEILING, W.; STARY, F.: Nanosecond Pulse Techniques. Berlin: Akademie-Verlag 1969

THE DIONYSOS SATELLITE RANGING LASER, 1978

W.C.Johnson and G.Veis
Dionysos Satellite Tracking Center

The Dionysos satellite laser ranging system has been improved since previously reported, (1), to increase it's rate range and accuracy. Work is in progress to further increase it's ranging rate, it's measuring accuracy and to automate the system with computer control.

A new laser has been installed to replace the previous 1 joule, rotating prism Q-switched ruby laser. The new laser was manufactured by Holobeam Laser presently of Orlando, Florida, U.S.A. This laser is water-cooled and has a single ruby rod, 6"x1/2"dia. with a hellical flash lamp. The rod output is Q-switched by a Pockels cell producing an output energy of 4.5 joules with a half energy divergence of less than 7 milliradians and a half amplitude pulse width of 25 nanoseconds. Included with the laser is a Pockels cell pulse slicer. The output energy after slicing is approximately 0.75 j. with a half amplitude pulse width of 7 nsec. This slicer will be used routinely in the near future.

The laser is installed on an optical bench in the control room and the output is directed by prisms into the altitude-azimuth (fig.1) mount above this room. In the transmitting telescope, the divergence can be adjusted to less than 1 mrad. The laser is capable of a firing rate of 60 pulses per minute at it's maximum energy, however in 1977, the laser was routinely used at 8 ppm.

The Coude' alignment of the laser ranging mount output was first used in 1977. The previous laser was mounted directly in the transmitting telescope. The mount is driven by stepping motors in altitude and azimuth in steps of 0.001 degree. The pointing accuracy of the mount and attached receiving telescope is $\pm$0.003 degree of $\pm$10 arcsec. However the overall pointing accuracy of the transmitted beam after passing through the mount and transmitting optics is presently only $\pm$1 arcmin. Routine ranging with returns from all parts of the sky has been done with a laser beam diverence of 1 mrad. Work is in progress to improve output pointing to allow reduced output divergence.

To accommodate the increased ranging rate of 8 ppm, several changes were made to the control electronics (fig.2). Previously, the difference in altitude and azimuth to the next position for the mount and the predicted range delay were entered manually for the 2 ppm ranging rate. Presently, a paper tape, generated by the prediction program, provides the necessary input to track and range for each satellite pass at the 8 ppm rate.

Current work is aimed at entry of the prediction parameters through a 9825A Hewlett-Packard computing calculator (fig.3). This calculator will control the system during operation and handle the input and output of data. Connection will be made by telephone data link to the maine computer in Athens. This connection will transfer orbital elements as received at Dionysos from the Smithsonian Astrophysical Observatory and the satellite pass predictions as generated by the computer in Athens. The predictions will be recorded on magnetic cassettes and the calculator will drive the system through each pass with various adjustments possible by the observer. Returns data will be recorded together and other auxiliary information on cassette and summaries prepared by the calculator.

The ranging rate will be increased to 20 ppm in the planned system. The rate will not be fixed, but will vary within each pass. This will allow maximum pass coverage within the limits of the mount drives speeds. The calculator will record also the local temperature, pressure and relative humidity from sensors at the time of each observation.

The addition of the pulse slicer in the laser output will require improvement of the pulse detection instrumentation. Presently, the range counter uses fixed thresholds for starting and stopping. The stop pulse is derived from the received pulse after operator controlled attenuation. It is planned to use an analog system of pulse discriminators for pulse detection similar to that presently used in the SAO tanging systems,(2).

Successful measurements during 1977 using the system shown in figures 1 and 2 are totaled in the next table. The measurements had approximately an accuracy, of better than a meter.

DIONYSOS LASER

SUCCESSFUL MEASUREMENTS* (1977)

	BE-3	GEOS I	STARETTE	GEOS III	TOTALS
June	-	3(1)	-	-	3(1)
July	-	45(9)	-	85(14)	130(23)
August	555(22)	310(15)	439(31)	284(15)	1588(83)
Sept.	12(1)	36(1)	138(12)	151(7)	337(21)
Oct.	336(12)	74(4)	-	191(8)	601(24)
Nov.	-	4(1)	-	4(1)	8(2)
					2667(154)

* Numbers refer to successful return.
Number in parenthesis successful passes.

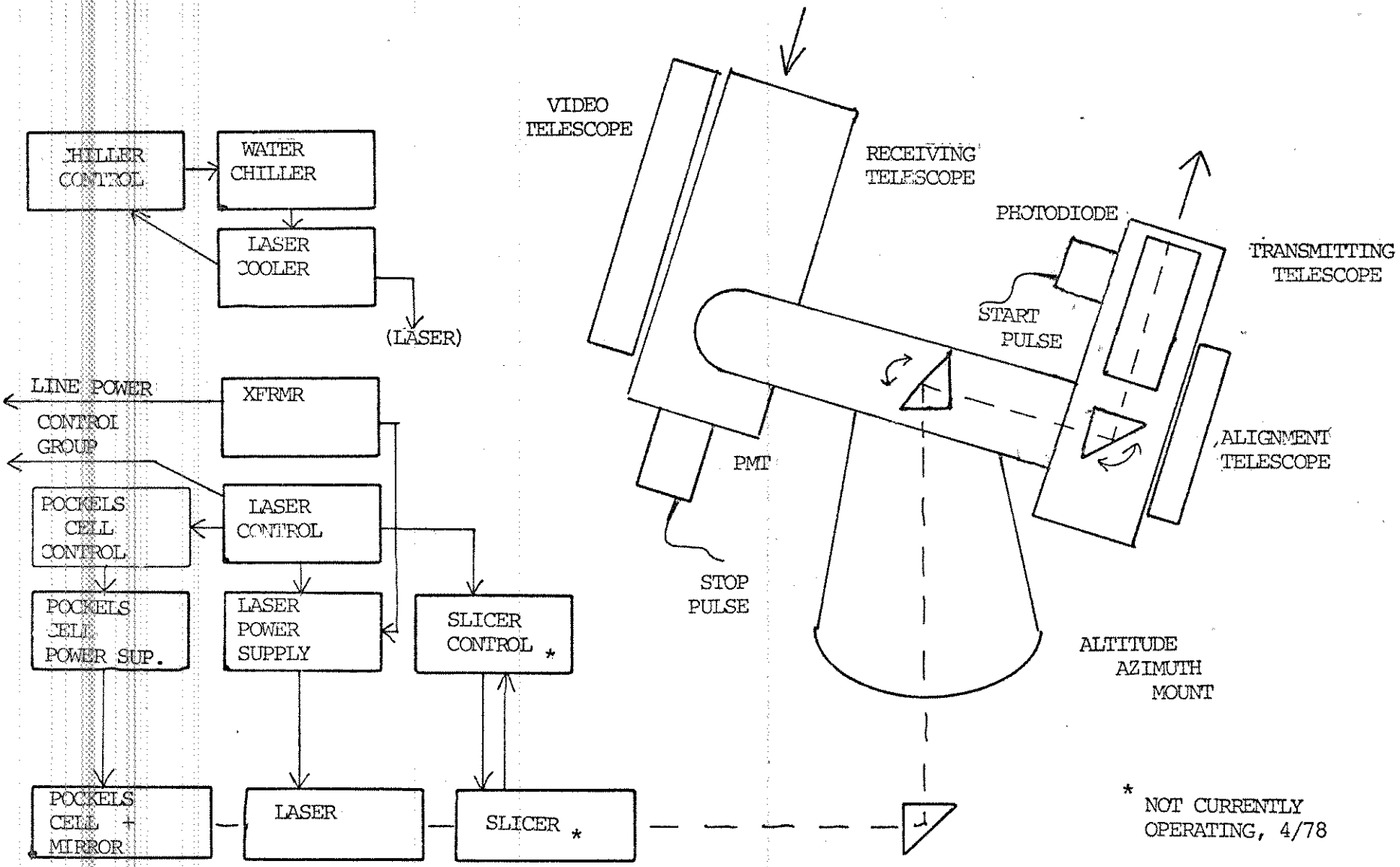

DIONYSOS LASER - LASER GROUP AND MOUNT GROUP

(FIG.1)

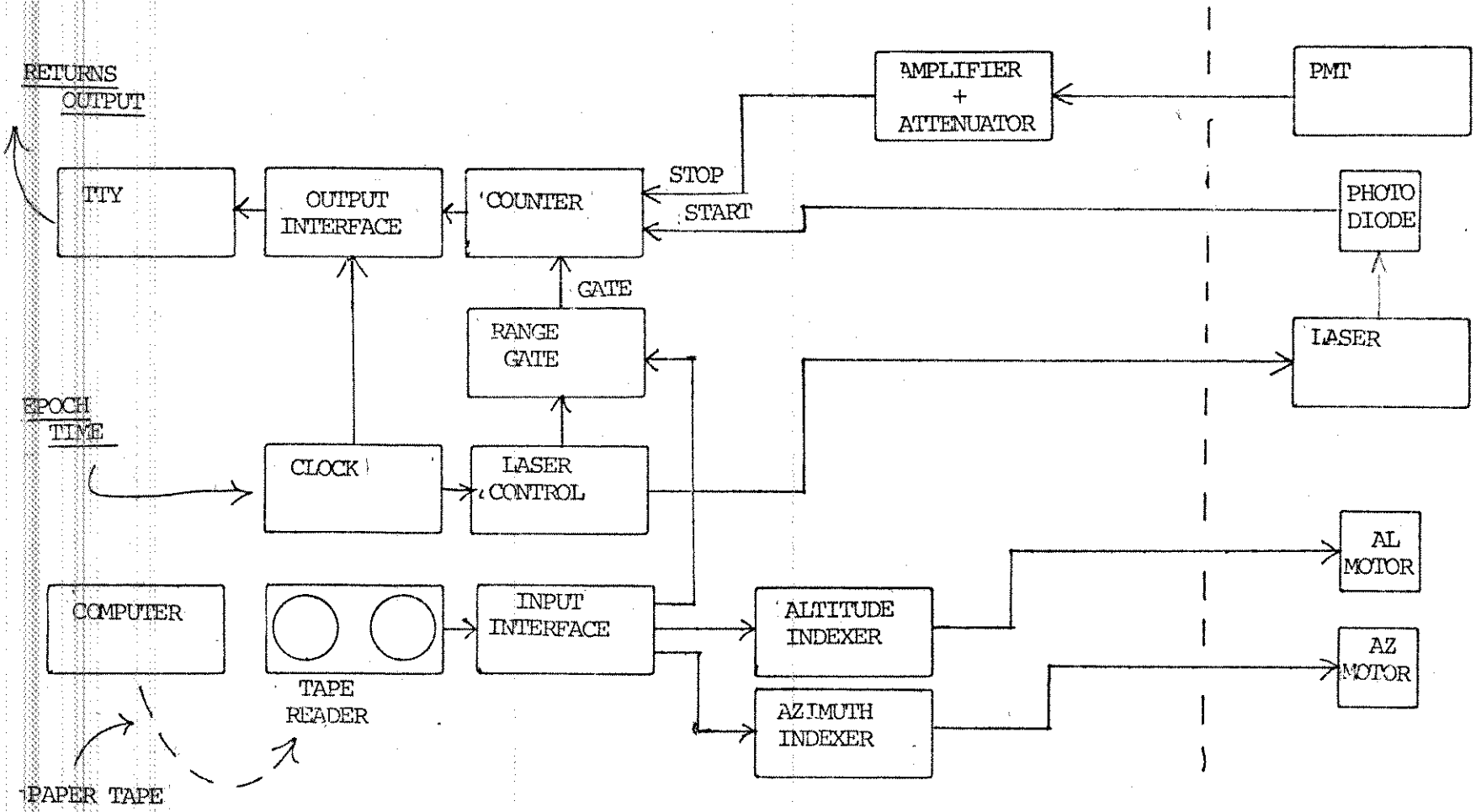

DIONYSOS LASER - CONTROL GROUP (CURRENT, 4/78) (FIG.2)

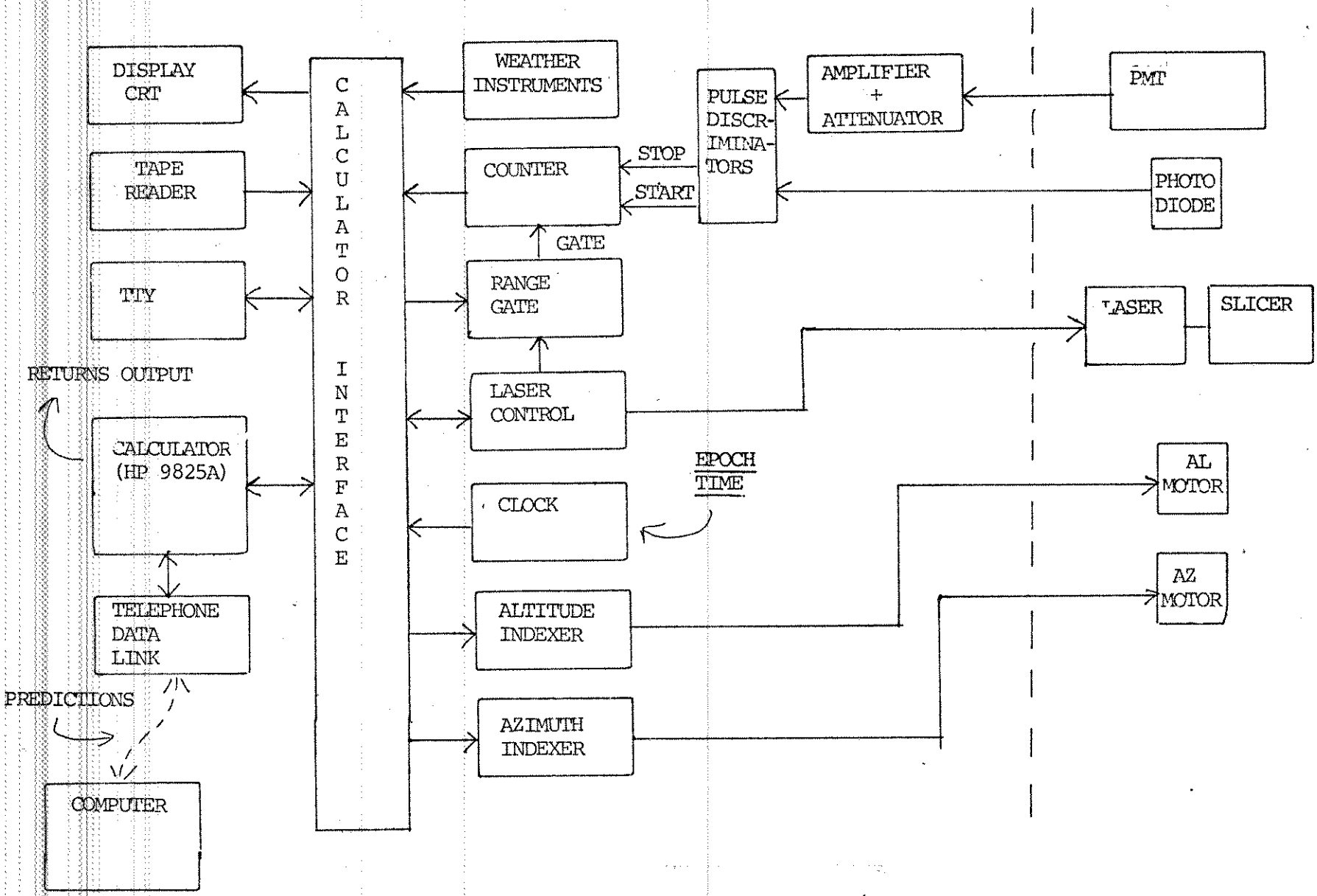

DIONYSOS LASER - CONTROL GROUP (WORK IN PROGRESS)

(FIG. 3)

References

(1) G.A.C.Assimakis, D.D.Balodimos, G.Veis : "THE LASER SATELLITE RANGING SYSTEM AT THE DIONYSOS STATION" Proceedings of the International Symposium on the Use of Artificial Satellites for Geodesy and Geodynamics, Athens, (1973).

(2) M.R.Pearlman, C.G.Lehr, N.W.Lanham and J.Wohn : "THE SMITHSONIAN SATELLITE RANGING LASER SYSTEM" Proceedings of the Second Workshop on Laser Tracking Instrumentation, Prague (1975).

THE SATELLITE LASER RANGING SYSTEM AT CAGLIARI OBSERVATORY

L. Cugusi
Istituto di Astronomia
Università di Cagliari - Italy

INTRODUCTION

The laser ranging station of Cagliari Observatory was originally conceived in 1975 as an improved first generation system. Its ranging capabilities are estimated to allow to easily track the recently launched geodynamic satellites as Starlette and Geos 3.

The main scientific aim is to study polar motion and Earth's rotation by means of the satellite observational data collected. Indeed laser range observations will join at Cagliari Observatory more conventional observational techniques for geodynamic studies: VZT (operating at Carloforte since 1889), PZT (now undergoing the final testing), Doppler receiver (operating from last year) and Danjon Astrolabe (operating by the end of this year).

STATION DESCRIPTION

1. LASER TRANSMITTER SYSTEM

The optical rail assembly (Apollo Lasers) consists of a 3"x3/8" (7.5 x1 cm) ruby oscillator, which is operated in the Q-switched mode, giving about 1 J in 20-25 ns pulse width at 30 pulses per minute.

The output of the oscillator is fed into a KD*P Pockels cell and polarizer combination, which forms an electro-optic shutter (with laser-triggered spark gap) to chop the Q-switched pulse. The output of the shutter drives a 6"x1/2" (15x1.3 cm) ruby amplifier: typical final output is 1 J in 5 ns pulse width at 30 ppm, or 200 MW peak power. The beam divergence reaches the relatively high value of 3 mrad, typical of the multimode resonant cavities.

A power supply provides pulsed energy to the flashlamps and Pockels cells. A control console includes electronics for controlling bank voltage, lamp triggering, Q-switch triggering and timing.

Both the laser heads are cooled by means of a refrigerated water-to-air system, which provides temperature controlled coolant water.

A laser energy meter and a vacuum photodiode together with a 500 MHz real-time-bandwidth oscilloscope permit to monitor the laser output.

The optical rail is supported by a granite slab, resting on a concrete foundation. The laser beam reaches the collimating telescope through a coudé optical path of five multidielectric layer coated flat mirrors.

The collimating telescope is a 6x Cassegrain quasi-afocal optical system; so the beam divergence should be at least 0.5 mrad.

2. TRACKING SYSTEM

The turret is an EOTS-B Cinetheodolite with a rebuilded optical section. Blind tracking is not jet possible (future tracking improvements are described in the last section): after sunset and before sunrise observing satellites is possible through a TV system, by controlling both azimuth and elevation motors of the mounting by means of a joy-stick.

The TV system consists of a camera tube (RCA 4804) for very low light level, controlled by a custom-built camera control unit,

installed at the first focus of a 25 cm diameter Maksutov type telescope: the focal lenght of the telescope was chosen to give a 2° field of view on the TV monitor. Objects as faint as 12th magnitude fall within the capabilities of this TV system.

3. ECHO RECEIVER AND DATA RECORDING SYSTEM

A telescope of 50 cm diameter collects and focalizes the weak echoes, through a suitable filtering optical system, on the photo cathode of a Quantacon type (RCA C31034) photomultiplier. This photomultiplier is estimated to be very suitable only for night-time ranging.

Both the laser output pulse and the satellite echo reach the photomultiplier: indeed a fiber optic shunts a small fraction of the output pulse to the photomultiplier; so that only one discri mination circuit is necessary.

The anode pulses are amplified externally before discrimination is feasible in practice: a low noise, fast amplifier (ORTEC 454 TFA) has been chosen.

The discrimination is carried out by means of a constant fraction timing operation (ORTEC 473 CFD), intended to avoid that timing depend on pulse height.

The output of the discrimination circuit is a shaped pulse which trigger (start pulse) both the time interval counter (Eldorado 796, 1 ns resolution) and the preset counter (see block diagram) and allow the printing of the content of the clock register. Any pulse discriminated before preset time has elapsed is considered to be the expected satellite echo (stop pulse): it stops the time interval counter and allow the printer to record the time-of-flight. On the contrary any signal crossing the discriminator threshold after the preset time will not generate an output.

4. TIMING AND TIME SYNCHRONIZATION

A cesium master clock (Oscilloquartz B 3200) provides 1 MHz external frequency to the time interval counter; it controls also the clock register, giving 1 μs resolution.

Time synchronization is carried out by means of both Loran-C and TV techniques. In the former case, time signals of the Simeri Crichi station are usually received; in the latter, a mutual data exchange takes place with the Institute "Galileo Ferraris" of Turin.

In the best conditions, it seems possible to obtain time synchronization within less than 1 μs.

5. EXPECTED SYSTEM RANGING ACCURACY

A theoretical evaluation (L.Cugusi et al., 1975) of the final accuracy of the range data collected by means of a laser ranging station like that described, shows that a value close to 20 cm should be obtained. Nevertheless it is only a rough estimate, this value depending strongly on the height of the return signals, calibration techniques and system internal stability.

6. FUTURE IMPROVEMENTS

In the near future, priority will be given to blind tracking: real time tracking will be obtained by interfacing the Cinetheodolite electronics with our minicomputer (Honeywell Series 60, Mod. 6/43, 64 KB Memory). Another interface will allow to record on the magnetic tape unit of the minicomputer the observational data.

REFERENCES

L.Cugusi, F. Messina, E. Proverbio, A Laser Range Tracking Station for Geodynamis Satellites, Publ. Staz. Astron. Intern. Latit. Carloforte-Cagliari, N°51, 1975.

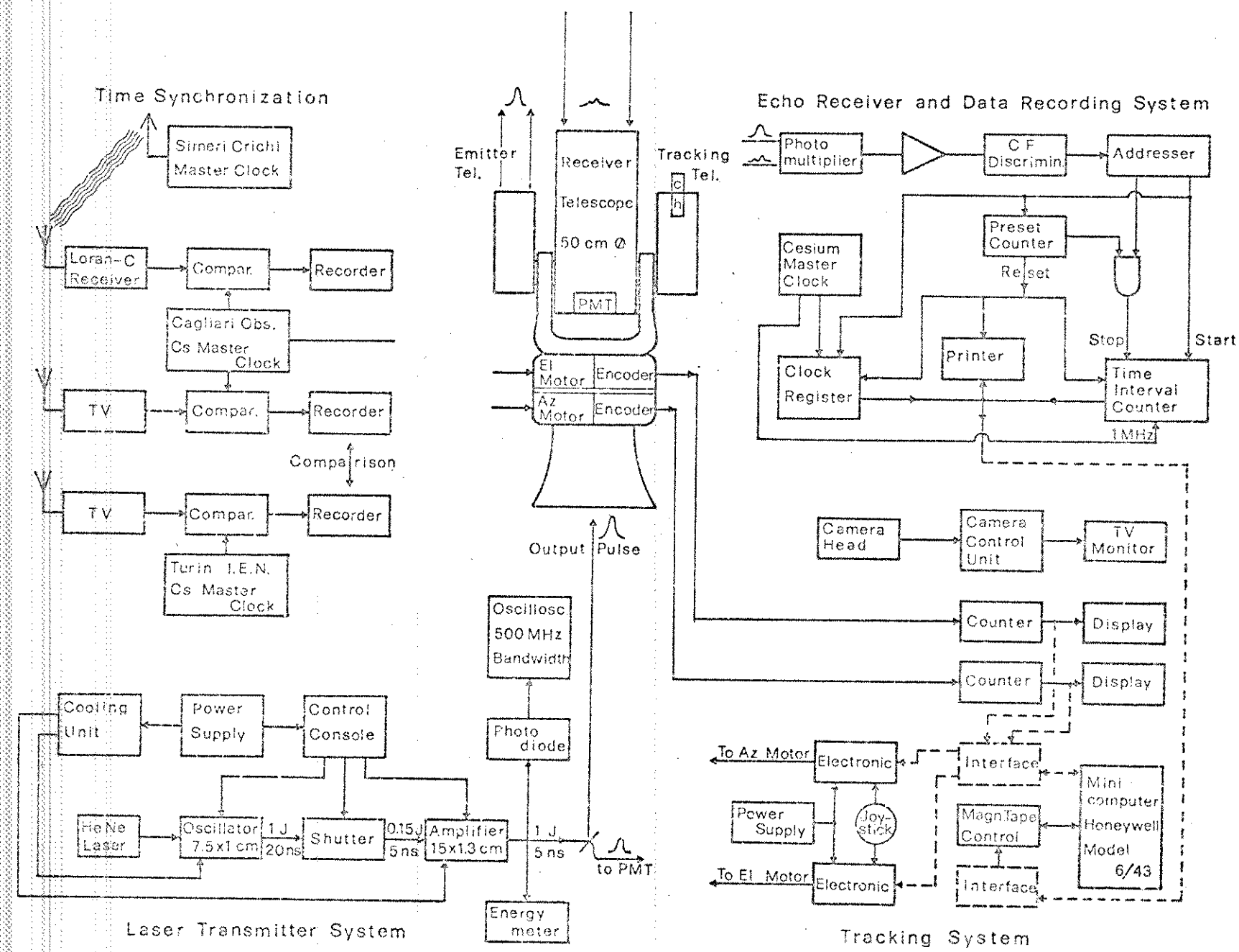
Time Synchronization
Simeri Crichi Master Clock
Loran-C Receiver
Compar.
Recorder
Cagliari Obs. Cs Master Clock
TV
Compar.
Recorder
Comparison
TV
Compar.
Recorder
Turin I.E.N. Cs Master Clock
Emitter Tel.
Receiver Telescope 50 cm Ø
Tracking Tel.
PMT
El Motor
Encoder
Az Motor
Encoder
Output Pulse
Echo Receiver and Data Recording System
Photo multiplier
C F Discrimin
Addresser
Preset Counter
Reset
Cesium Master Clock
Printer
Stop
Start
Clock Register
Time Interval Counter
1 MHz
Camera Head
Camera Control Unit
TV Monitor
Counter
Display
Counter
Display
Oscilliosc 500 MHz Bandwidth
Photo diode
Energy meter
Cooling Unit
Power Supply
Control Console
He Ne Laser
Oscillator 7.5x1 cm
1 J
20 ns
Shutter
0.15 J
5 ns
Amplifier 15x1.3 cm
1 J
5 ns
to PMT
Laser Transmitter System
To Az Motor
Electronic
Interface
Power Supply
Joy-stick
Magn.Tape Control
Mini computer Honeywell Model 6/43
To El Motor
Electronic
Interface
Tracking System

THE ZIMMERWALD SATELLITE RANGING STATION
TECHNICAL DESCRIPTION

I. Bauersima, G. Beutler, W. Gurtner, P. Klöckler, M. Schürer
Astronomisches Institut der Universität Bern
Bern, Switzerland

This report contains a technical description of the Zimmerwald Laser Observatory, as it has been constructed from 1975 to 1978. In the second section we state the evolution taking place during 1978. In the final section the planned completion works for the years 1979 - 1981 are listed.

TECHNICAL DESCRIPTION OF "STATUS QUO"

(see diagram)

Ruby Laser System

Energy	3 - 5 joules
Halfenergy pulse width	15 - 20 nsec
Natural beam divergence *)	3.5 mrad
Beam divergence, when leaving the telescope	0.7 mrad

Dye Laser System

Energy	12 Joules
Natural beam divergence	10 mrad
Beam divergence, when leaving the telescope	2 mrad
Halfenergy pulse width	some µsec

The Telescope

Biaxial horizontal mounting
Both axes are driven by stepping motors with a resolution of
2.7 arcsec in elevation
5.4 arcsec in azimuth
Maximum velocities: 2,5°/sec in elevation
5,0°/sec in azimuth

*) Beam divergence: Angle between axis and the outermost beam

Transmitting telescope (TT)

Three prisms to conduct the beam into the transmitting telescope. The lowest prism may be switched from the ruby to the dye system and vice versa.
The transmitting telescope is a Galilei-telescope opening the beam 5:1.

Tracking and receiving telescope (RT)

Main mirror (spherical), diameter: 52,5 cm. Triple lense system in front of the TV-Camera to correct for the sphericity of the mirror. The surface of the first lense reflects the ruby light via Barlow and Fabry lenses into the echo photomultiplier.
TV-Camera (Grundig FA 42 S): Allows the observation of objects up to the magnitude of 9.5.

Tracking

The picture of the TV-Camera is displayed on the TV-Monitor (diameter 55 minutes of arc). Direction and velocity of the telescope may be preselected and started automatically by the station clock. The image of the satellite can now be centered manually. The pointing accuracy in this mode of operation is limited by the resolution of the TV-System, which is 15 arcseconds.

Epoch Timing

A HBG-receiver ensures determination the epoch within $\sim$ 20 µsec.

Echo-detection

Is established by a photomultiplier RCA 7265 with S-20 cathode. In front of the photomultiplier there is a 10 Å interference filter. An electromechanical shutter and a digitally presettable range gate reduce the probability of error counts.
Light travelling time is measured by an "Eldorado 796" counter (Resolution 1 nsec).

Waveform analysis

The shapes of the outgoing and incoming pulses are photographically registered from a TEXTRONIX 556 oscilloscope. The measured flight time is then corrected to the respective centers of the pulses.

Data registration

Epoch time, light travelling time, approximate position of the telescope (azimuth, elevation) are printed on a HP 5055 A printer.

WORKS IN PROGRESS (1978)

Installation of a better TV-Camera (JAI 740 ISIT) permitting the observation of objects up to the magnitude of 15.

Installation of a PDP 11/40 Computer system with two disks and 32 k words of memory.
The system will take over the following tasks:

- data registration (replacing h), Section 1)
- Satellite predictions adapted to TV-tracking.

FUTURE PLANS (1979-1981)

- Computer tracking
- new epoch timing (accuracy ± 1 μs)
- reconstruction of transmitting telescope to allow for a variable beam divergence.

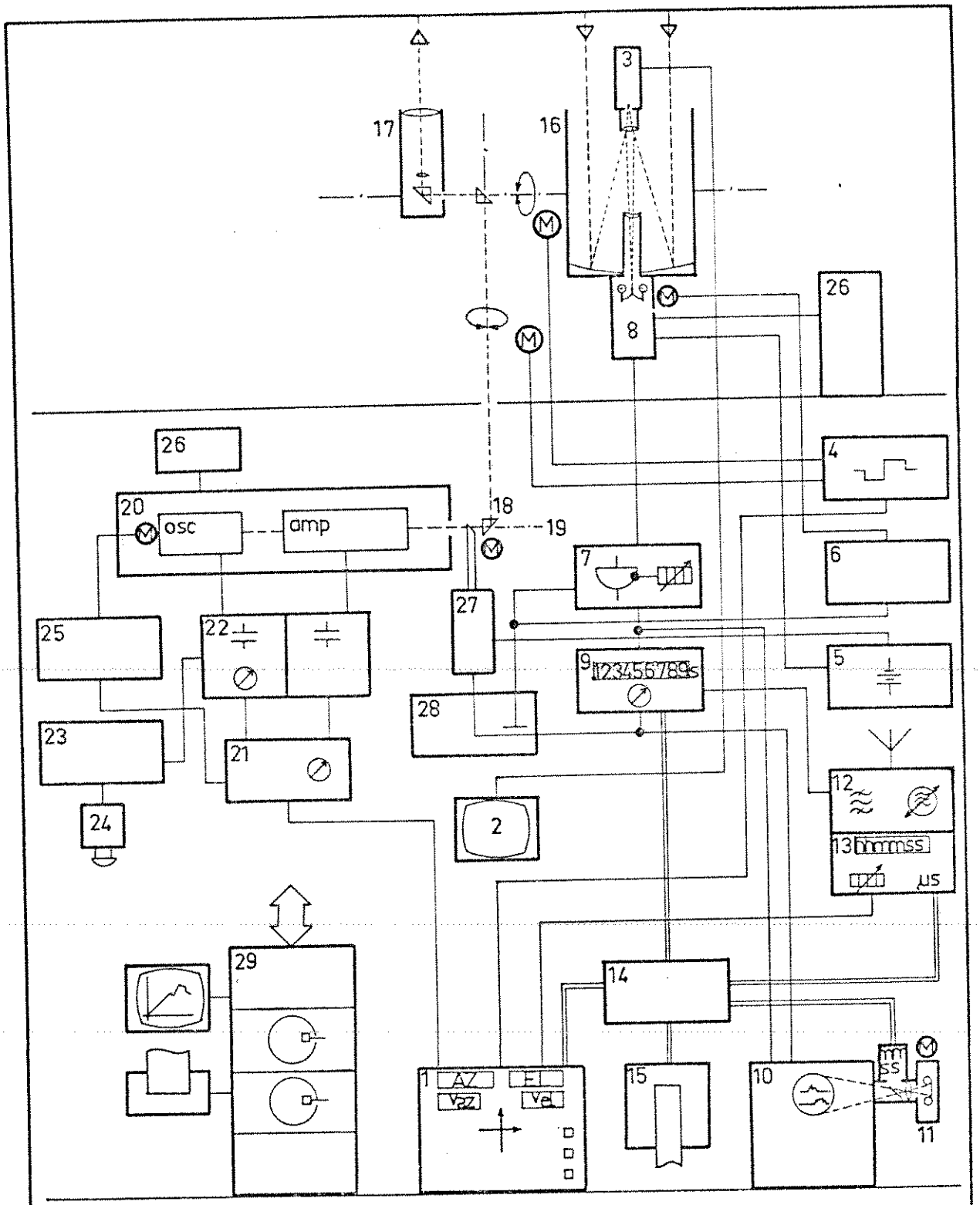

INDEX:

1 MANUAL CONTROL DESK
2 TV MONITOR
3 TV CAMERA
4 STEPPING MOTOR CONTROLS
5 PM POWER SUPPLIES
6 SHUTTER CONTROLS
7 RANGE GATE
8 STOP PM ASSEMBLY
9 FLIGHT TIME COUNTER
10 OSCILLOSCOPE
11 PHOTOGRAPHIC CAMERA
12 TIME SIGNAL RECEIVER
13 STATION CLOCK
14 DATA MULTIPLEXER
15 PRINTER
16 RECEIVING TELESCOPE
17 TRANSMITTING TELESCOPE
18 SWITCHING PRISM
19 DYE LASER
20 RUBY LASER
21 FIRING CONTROL
22 PUMPIMG POWER SUPPLY
23 STARTUP AND SAFETY UNIT
24 PANIC PUSHBUTTONS
25 ROTATING PRISM DRIVER
26 COOLING SYSTEMS
27 START PM ASSEMBLY
28 SIGNAL COUPLER
29 COMPUTER

ZIMMERWALD SATELLITE RANGING STN.

THE METSÄHOVI LASER RANGING SYSTEM

S.J. Halme, M.V. Paunonen, A.B.R. Sharma
Helsinki University of Technology, Espoo, Finland
J. Kakkuri and K. Kalliomäki
Finnish Geodetic Institute, Helsinki, Finland

1. INTRODUCTION

The Finnish-Swedish Satellite Laser range finder is located at the Metsähovi Space Geodetic Station (Lat. = 60°13'.2, Long. = 24°23'.9) approximately 40 km from Helsinki. System planning was initiated in 1972 with financial support from the Academy of Finland, and in 1974 a cooperation agreement was made with the Geographical Survey Office of Sweden, which has provided further funding. The ranging system is now fully operational and the first range determination to the Geos-3 satellite has been done. The detailed description of the existing apparatus is reported elsewhere /1/.

2. THE LASER RANGE FINDER

2.1. Laser transmitter

The electro-optically Q-switched ruby laser oscillator consists a water cooled diffusely reflecting head (Korad K1), a helical flashlamp, a 100 mm long x 9.5 mm dia. ruby rod, a KD*P Pockels cell (Lasermetrics, Inc. Model 813), a Brewster stack polarizer (Interactive Radiation Inc.), a dielectric rear mirror and a 26 % sapphire etalon as the front mirror. The optical length of the resonator is 500 mm. The charge storage capacitor, 400 µF/5kV, is charged to 0...5kV using a conventional inductively current limited step-up transformer-rectifier system. The repetition rate is limited to 1/6 Hz by the laser head, cooling system and the charging system. The output pulse length, Fig. 1., depends on the pumping level. The length normally used is 20 ns and the pulse energy 1J. The beam divergence is about 3 mrad. The output beam is collimated using a x7 inverted aspherical Galilean telescope. The divergence can be adjusted from 0.4 to 3 mrad by defocusing. The start pulse for the time interval counter is generated by using a light guide to sample the transmitted pulse via the rear mirror, followed by opto-electronic conversion using a fast silicon photodiode and an amplifier-filter combination. The temperature-controlled

laser housing is situated on top of the telescope mount.

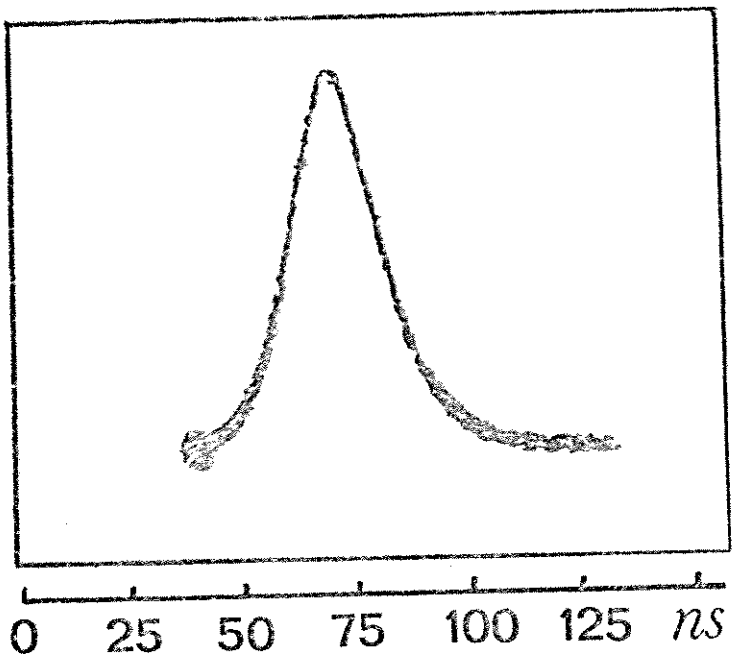

Fig. 1. Typical shape of the 25 ns long Q-switched ruby laser pulse.

2.2. Laser receiver

The return energy is collected using a 630 mm parabolic mirror with a focal length of 1730 mm. The 6 mm aperture of the electro-mechanical shutter, used for eliminating the near backscatter to the photomultiplier, defines a 3.5 mrad field of view. The background radiation is limited by a 3 nm interference filter with a transmission of 70 %. The light is collimated by a lens before it enters the filter. The photomultiplier used is an RCA C31034 which has a GaAs cathode with a quantum efficiency of 10 %, and a multiplier gain of $6 \cdot 10^5$ at 1680V. This photomultiplier is protected against excessive anode current and cathode voltage. Also an RCA 8852 with a multialkali cathode(quantum efficiency about 4 %) can be used, especially under twilight conditions or if a higher amplification (up to 10^8) is needed. The anode pulse is fed through a 12 m long coaxial cable to the electronic amplifier. To allow the use of the whole pulse for determining the range, the incoming pulse is integrated at the collector of a transistor amplifier with a long time constant.

The travel time of the light pulse is measured with a high resolution time interval counter (Nanofast 536B, modified), which has a nominal resolution of 25ps. Median detection, which uses an adaptive threshold and thus also

eliminates amplitude dependent time walk, is realized using the half-max plug-in of the counter (Nanofast M/2-unit). The random error of the counter system is about 0.15 ns(r.m.s.), while the systematic error is about 2 ns within the dynamic range of 0.3 V to 12 V.

Range calibration is performed using a 332 m calibration line. A typical set of 24 pulses is shown in Fig. 2.

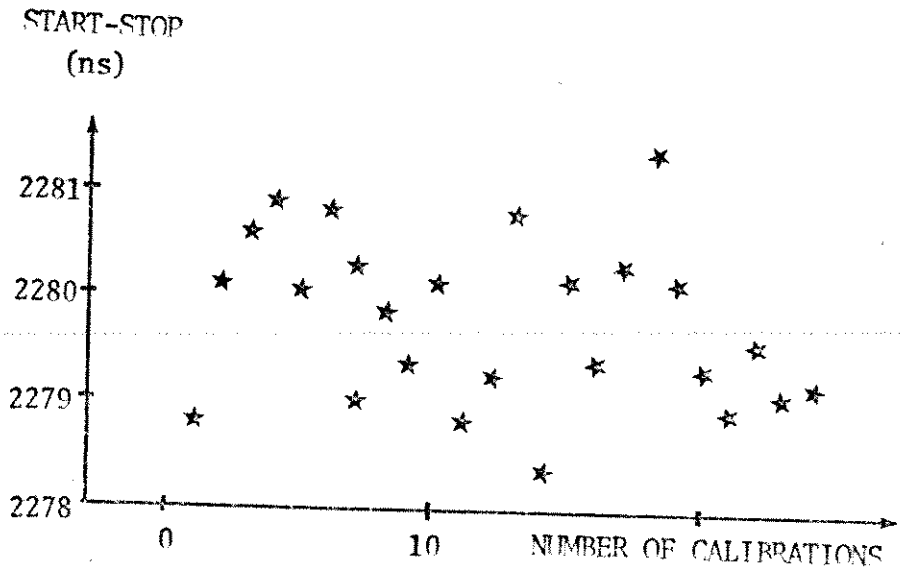

Fig.2. A calibration measurement. The average content of the return pulse was about 600 photoelectrons. The time interval between shots was 30 s. The standard deviation is 0.77 ns.

A transient digitizer (Tektronix R7912) is connected in parallel to the PMT anode cable, via a sampling resistor and an amplifier, to monitor the photomultiplier pulses.

2.3. Telescope mount and electronics

The telescope mount is equatorial and is sidereally driven, thus allowing easy calibration against known star positions. The mount, which is driven by stepping motors, is controlled by a minicomputer (D-116, Digital Computer Controls, Inc.). Position control is achieved using the open loop principle.

The pointing accuracy is better than ±0.6 mrad or ±2 min of arc. The satellite positions are calculated in advance on the basis of predictions, which are in the format of the AIMLASER programme. This programme has been received from Kootwijk /2/ and modified for the PDP 11/10 minicomputer at the Finnish Geodetic Institute.

The D-116 minicomputer gives the commands to the drive system to move the telescope to the correct position in advance of the expected arrival time of the satellite. The computer also fires the laser at the predicted time corresponding to the predicted direction. The firing times can be corrected during the satellite pass if needed e.g. after visual acquisition. Also manual speed and position control is possible using a joystick or thumbwheels. The resulting data are logged by the computer and include epoch of pulsing, nanosecond counter reading, right ascension, declination, air temperature, atmospheric pressure and relative humidity.

Station time keeping is achieved using a crystal clock which is phase locked to the LORAN-C transmission. In this way short term stability is provided by the crystal, while long term stability is assured by the atomic clocks used for controlling the LORAN-C. The accuracy obtained is between 1-5 μs.

The weather station is automatically operated using capacitive type transducers. The measurement accuracy has been found to be ±0.5°C for temperature, ±0.7 mb for air pressure, and ±3.9 % for relative humidity.

Two guiding telescopes are used for pointing purposes: a 30 mm auxiliary finder telescope with x 6 magnification, and a 203 mm Cassegrain telescope with a Schmidt plate (Celestron 8, f/10). The guiding telescope and the main parabolic mirror are aligned using a fixed star by detecting the increased anode current of the PMT. The laser transmitter is aligned towards the calibration target against marked positions corresponding to the relative positions of the guiding receiver and the transmitter telescopes. The laser beam spot at the target is well defined, and therefore its size and position can be adjusted against crossed marks.

3. CONCLUDING REMARKS

The accuracy of the present ranging system is estimated to be 1 m, as is common with other stations which are using Q-switched pulses. The instrumental resolution is about 0.5 ns which corresponds to 7.5 cm in range.